PARAMETERS AFFECTING CRITICAL HEAT FLUX OF NANOFLUIDS: HEATER SIZE, PRESSURE ORIENTATION AND ANTI-FREEZE ADDITION

by

MADHAV RAO KASHINATH

Presented to the Faculty of the Graduate School of

The University of Texas at Arlington in Partial Fulfillment

of the Requirements

for the Degree of

MASTER OF SCIENCE IN MECHANICAL ENGINEERING

THE UNIVERSITY OF TEXAS AT ARLINGTON

AUGUST 2006

ACKNOWLEDGEMENTS

I would like to thank my supervising professor Dr. Seung Mun You, for giving me the opportunity to work at the Microscale Heat Transfer Laboratory and be a part of his research activities. I would also like to thank my fellow laboratory members for having extended their support and for sharing their knowledge and helping me complete my study. Finally, I would like to thank my family and friends without whose support and encouragement I could not have accomplished this study.

AUGUST 1, 2006

ABSTRACT

PARAMETERS AFFECTING CRITICAL HEAT FLUX OF NANOFLUIDS:
HEATER SIZE, PRESSURE ORIENTATION
AND ANTI-FREEZE ADDITION

Publication No. _____

Madhav Rao Kashinath, MS

The University of Texas at Arlington, 2006

Supervising Professor: Seung Mun You

This research aims at investigating the effect of heater size, pressure, heater orientation and effect of anti-freeze addition on critical heat flux of nanofluids which have shown large potentials as coolants for high power generating uses. Nanofluids have shown about ~ 180 - 200% enhancement in critical heat flux values. The effect of heater was carried out using three different sized heaters. Maximum enhancement of ~190% was achieved for a 1×1 cm^2 heater. The effect of pressure on critical heat flux was investigated by testing nanofluids at three pressures. Maximum enhancement of ~ 240% increase in critical heat flux was observed at the lowest pressure tested. Surface

orientation effect on critical heat flux carried out for a 2 × 2 cm^2 heater at five orientations revealed about ~120% enhancement over the critical heat flux obtained using Zuber's correlation at an orientation of 150°. Two commercially used antifreezes, ethylene glycol and propylene glycol, were used to study the effect of anti-freeze addition to nanofluids. Alumina-water nanofluid of 0.025 g/L concentration mixed with the antifreezes at five compositions by volume showed a maximum enhancement of ~120% for ethylene glycol and ~70% for propylene glycol.

TABLE OF CONTENTS

LIST OF ILLUSTRATIONS

NOMENCLATURE

A_H	area of the heater surface, [m^2]
C_{pl}	specific heat, [J/kg.K]
h_{fg}	latent heat of vaporization, [J/kg]
L'	dimensionless length
L	length, [m]
N_j	number of vapor jets on the surface of heater
q''_{CHF}	critical heat flux, [kW/m^2]
r, s	constants bearing values 0.33, 1.0 respectively for water
T_{wall}	temperature of the heater surface, [°C]
T_{sat}	saturation temperature, [°C]

Greek symbols

Δ	difference
λ	wavelength of vapor jets, [m]
μ	dynamic viscosity, [$N.s/m^2$]
σ	surface tension, [N/m]
ρ	density, [kg/m^3]

CHAPTER 1

INTRODUCTION

Progress of technology towards smaller sizes in the field of electronics is being confronted by the problem of heat dissipation due to the limitations of current techniques to dissipate high powers from the areas much smaller than the previous decade. Extensive research is being done to provide solutions to the problem of heat dissipation from small areas such as chips. Two-phase boiling heat transfer is one such area which is being studied for solutions to the problems being faced in today's electronic cooling industry. Delaying the occurrence of critical heat flux (CHF), which is one of the important phenomena of boiling, is being researched. Surface roughness techniques to enhance the nucleate boiling heat transfer have been developed and shown to provide ~300% enhancement over plain surfaces by Chang and You [1]. Moreover, conventional working fluids for boiling are being replaced with newer liquids developed for the purposes of electronic cooling. In the recent past, nanofluids have shown promise of cooling high powers due to higher critical heat fluxes compared to water.

Critical heat flux is known to be a limiting factor for heat dissipation in two-phase boiling heat transfer. During the process of boiling; after bubble incipience, nucleate boiling occurs, during which fresh liquid reaches the surface of the heater without much resistance from the vapor formed at the surface of the heater. This process continues and transforms into fully-developed boiling wherein the bubbles

formed are larger than the preceding stage. After a certain heat flux is reached, the vapor forming at the surface of the heater envelops the entire surface of the heater. This blanketing of the surface causes the temperature of the surface to drastically increase from the previous states; moreover the bulk liquid faces a much greater thermal resistance from the vapor in reaching the surface of the heater. This point or heat flux at which the temperature of the surface sees a sudden rise in temperature is called as critical heat flux.

One of the problems being faced in boiling heat transfer cooling applications is the occurrence of critical heat flux. Temperatures at the point of occurrence of critical heat flux are high enough to damage the devices and therefore, methods to increase CHF are being investigated. Nanofluids, consisting of nano-sized particles dispersed in solutions, have shown to have great potential due to their ability to reach higher critical heat fluxes than water or most of the other liquids. The ability of nanofluids to delay the occurrence of critical heat flux is the main motivation for this study, which aims at further understanding behavior of nanofluids for parameters of heater size, pressure, orientation and addition of anti-freeze.

1.1 Literature Review

1.1.1 Nanofluids Related Review

Nanofluids have recently shown promise in enhancing heat transfer properties. Lee et al. [2] conducted tests of dispersing copper oxide and aluminum oxide in water

and ethylene glycol and found enhancement in the thermal conductivity compared to pure liquids, they obtained maximum enhancement at 4% by volume concentration of copper oxide nanoparticles in ethylene glycol. Eastman et al. [3] further reported 40% enhancement in thermal conductivity on dispersing 0.3 % by volume of copper nanoparticles in ethylene glycol. Choi et al. [4] conducted test for thermal conductivity of nanofluid with carbon nanotubes dispersed in oil and found a great increase in the thermal conductivity compared to the theoretical predictions, leading to the hypothesis that not only spherical shaped particles (as used by earlier researchers) but particles of other geometries also enhance the thermal conductivity. More recently Liu et al. [5] have reported similar results of increase in thermal conductivity by about 24 % using copper nanoparticles dispersed in water. However, they have also reported that the increase in thermal conductivity reduced with time.

Das et al. [6] were among the first researchers to report on the behavior of nanofluids when used as working fluids for boiling. Das et al. [6] found that the boiling heat transfer coefficient degraded with increase in alumina nanoparticle concentrations in water ranging from 0.1% to 4% by volume. They tested alumina (Al_2O_3) nanoparticles dispersed in water using a 20 mm diameter cartridge heater. To better understand the behavior of decrease in heat transfer Das et al. [7] tested the same composition of nanofluids with smaller sized heaters, Das et al. [7] again reported a decrease in the boiling heat transfer coefficient with increase in concentration of nanoparticles. They attributed the decrease in heat transfer to the “smoothening” of the heater surface due to deposition on nanoparticles into surface cavities.

You et al. [8], reported up to 200% enhancement in q''_{CHF} on dispersing 0.025g/L of alumina nanoparticles in water, without any change in the heat transfer coefficient. Similar results as those obtained by You et al. [8] were obtained by Vassallo et al. [9] who tested with silica nanoparticles dispersed in water. Pioneering work on bubble size, departure frequency and effect of heater surface orientation of nanofluids was reported by Kim et al. [10] for small square copper heater. Recently Moreno et al. [11] reported similar trends in higher q''_{CHF} due to the addition of zinc oxide (ZnO) nanoparticles to water. They also reported a 120% increase in the q''_{CHF} of aqueous ethylene glycol based nanofluid at 0.025g/L concentration of alumina nanoparticles.

1.1.2 Effect of Heater Size on Critical Heat Flux

Critical heat flux of fluids as a function of heater size has been investigated extensively. Kutateladze and Gogonin [12] conducted experimentation by varying the heater size to estimate the effect on q''_{CHF} of ethyl alcohol at an orientation of 0° (horizontal, facing upwards) and did not observe any change in q''_{CHF}. Ishigai et al. [13] reported a reduction in q''_{CHF} with increase in heater size for a cylindrical heater when tested with water as the test fluid. Similar results of reduction in q''_{CHF} with increase in heater size were reported by Kutateladze and Gogonin [12]. Lienhard et al. [14] experimented with various fluids for cases of submerged circular heaters and small size heaters forming the base of a fluids tank and observed that q''_{CHF} decreases with increase in heater size up to a point after which the reduction in q''_{CHF} would be less affected by the size of heater. Lienhard et al. [14] attributed this phenomenon of

decrease in q''_{CHF} to the number of "vapor jets" that can be present on the heater's surface area. Lienhard and Dhir [15] investigated effect of heater size by using ribbon heaters by making the long dimension as the horizontal and short as the vertical side and they reported a reduction in the q''_{CHF} with an increase in heater size. On testing for the effect of heater size on q''_{CHF} with FC-72 as working fluid, Saylor et al. [16] found that q''_{CHF} decreases rapidly with increase in size for smaller size heaters and remains relatively constant for larger sized heaters. The dimensionless L' after which the size of the heater does not seem to cause large changes in the q''_{CHF} is known as 'transition L''. McNeil and Bar-Cohen [17] determined that the transition point for FC-72 was L'_{trans} = 20 while testing for effect of heater size on the q''_{CHF}. McNeil and Bar-Cohen's claim was supported by Rainey and You [18] when they tested heaters up to the size of 25 cm^2 in saturated FC-72. Recently, Kim et al. [19] in their investigation on the effect of heater size on the q''_{CHF} using wire heaters of 25, 75, and 390 μm diameters observed the same effect of reduction in q''_{CHF} with increase in wire diameters. Kim et al. [19] concluded that this is due to the higher latent heat contribution by the wire of 390 μm diameter compared to 25 μm wire leading to a reduction in the micro-convection.

1.1.3 Effect of Pressure on Critical Heat Flux

The effect of variations in pressure on q''_{CHF} has been well documented for various kinds of fluids and flat surface heaters in the literature. Cichelli and Bonilla [20] studied the effect of pressure on the nucleate boiling of liquids such as water, ethanol, benzene and propane. They concluded that with an increase in pressure, the critical heat

flux increases up to a certain pressure (mostly up to one third of the critical pressure) and then starts to reduce. Abuf et al. [22] observed that at low pressures their plain heater did not match the q''_{CHF} predicted using Zuber's correlation [37] instead it "leveled off", when they tested for the effect of pressure on the q''_{CHF} with finned surfaces and plain copper tubes. Nishikawa et al. [23] studied for the effect of pressure on the heat transfer coefficient during boiling. Their testing using Freon, R11, R113, R21 and R114 showed mostly the same results of increasing heat transfer coefficient with increase in pressure. Mudawar and Anderson [24] observed similar results as other researchers that, with increase in pressure, the nucleate boiling heat transfer would increase and so would the q''_{CHF}. Luke [25] showed a similar trend of increase in the nucleate boiling heat transfer and increase in q''_{CHF} with increase in pressure. Recently, Rainey et al. [26] observed the same trends of an increase in q''_{CHF} with increase in pressure for their tests with FC-72 and microporous coated pin-finned surfaces.

1.1.4 Effect of Orientation on Critical Heat Flux

The heater surface configuration has been shown to be an important parameter affecting q''_{CHF}. Githinji and Sabersky [27] were among the first to study the effect of heater surface orientation on q''_{CHF} using a thin heating surface of 102 mm × 3.2 mm in water. They observed that q''_{CHF} increase with increase in orientation from 0° to 90°. Marcus and Dropkin [28] observed the same results on increase in heat transfer coefficient with increase in orientation from 0° to 90°. They attributed this behavior to the increase in agitation of the superheated boundary region due to the growth and

departure path length of the bubbles on the surface. They hypothesized that after a certain heat flux the heat transfer coefficient would not be affected by the orientation. Nishikawa et al. [29] confirmed the existence of this transition point after which the heat transfer coefficient would not be affected by the surface orientation. Chang and You [33] tested for the effect of orientation on q''_{CHF} using a small copper heater for FC-72 and observed trends similar to that of Githinji and Sabersky [27] of increase in q''_{CHF} as the surface orientation increases from 0° to 90° but saw a reduction in the q''_{CHF} on further increasing the orientation angle from 90° to 180°. Rainey and You [18] reported similar trends as Chang and You [33] for tests with FC-72.

Recently Kim et al. [10] tested the effect of orientation in nanofluids with a small copper heater of 1 × 1 cm^2 size and observed mostly the same behavior of increase in heat transfer coefficient due to increase in orientation angle from 0° to 90° and on further incrementing the orientation they observed reduction in q''_{CHF} and variations in the heat transfer coefficient.

1.1.5 Effect of Anti-Freeze Addition on Critical Heat Flux

Ethylene glycol (EG) is extensively used in heat transfer applications. Frea et al. [34] showed at 50% and 75% concentration by weight of ethylene glycol observed reduction in q''_{CHF} compared to pure ethylene glycol and pure water. Similar results of reduction in q''_{CHF} due to addition of ethylene glycol to water were observed McGillis and Carey [35]. In both the studies a reduction in the q''_{CHF} and deterioration of nucleate boiling heat transfer was observed. Investigations of Van Wijk et al. [36] with ethylene

glycol and water showed negligible or no change in q''_{CHF} of the mixture up to concentrations of 80% by weight. Similar results of negligible change in q''_{CHF} of a mixture of ethylene glycol and water up to 30% concentration by volume were reported by Moreno et al. [11]. In their study, Moreno et al. [11] saw that, with increase in ethylene glycol concentration up to 30 % by volume the q''_{CHF} of ethylene glycol based nanofluids reduced. However, although there is a reduction in the q''_{CHF} of ethylene glycol based nanofluids there is enhancement in q''_{CHF} of the mixture when compared to a mixture of ethylene glycol and water. Moreno et al. [11] reported that nanofluid + ethylene glycol mixture showed enhancement of about 130% over the q''_{CHF} calculated by Zuber's equation for q''_{CHF}.

1.2 Aim of Current Research

Previous research on nanofluids in boiling heat transfer has found that nanofluids provide enhancement in critical heat flux compared to that of water. This study aims at investigating some of the parameters that have shown to have influence on the critical heat flux. Experimental investigations on the effect of heater size, the effect of variations in pressure, the effect of orientation and the effect of adding anti-freezes (ethylene glycol and propylene glycol) on the q''_{CHF} of nanofluids will be carried out.

The research aims to test the above mentioned parameters and compare the behavior of nanofluid to the behavior of other fluids used in boiling heat transfer, in the hope of finding reasons for enhancement in q''_{CHF} observed due to addition of nanoparticles to

water and water based fluids.

This research also aims at further broadening the scope of research conducted by Moreno et al. [11] by conducting experiments with nanofluids and ethylene glycol mixtures up to concentrations of 50% by volume, in similar methods to that reported by Moreno et al. [11]. As a further study this research also aim at testing the effect of adding propylene glycol to water and water based nanofluid to the study the effect of additives on the q''_{CHF} of alumina-water nanofluid.

CHAPTER 2

EXPERIMENTAL APPARATUS AND PROCEDURE

2.1 Boiling Section and Test Heater

2.1.1 Test Section

The test apparatus is similar to that used by Moreno et al. [11] for all present tests. The apparatus is 20 cm (wide) × 20 cm (high) × 12.5 cm (depth), having 1.27 cm thick glass windows on the front and back to provide for viewing of boiling on the heater surface. Test vessel was made air tight to avoid inflow of non condensable gases after the degassing process and to prevent loss of pressure during tests. Two 12.7 mm diameter cartridge heaters were provided, within the vessel, for heating of the test fluid to saturation temperature. A heater stand made of aluminum had the provision to rotate the base at 15° increments from 0° to 90°, on which the heater is mounted, for testing at various orientations. Band heaters were externally attached to the test section to maintain the saturation temperature of the fluid during tests. The test section was provided with two valves, one on the top and one at the bottom. The bottom valve was used to drain the fluid after testing, whereas, the top valve was used to vent the non condensable gases dissolved in the fluid to an external condenser, which was connected to a chiller. Test liquid and vapor temperatures were measured using T-type thermocouples attached to the top plate of the vessel. Pressure in the vessel was

recorded using a pressure transducer. A schematic of the test vessel that was used for the pool boiling tests is shown in Figure A.1 (a).

2.1.2 Test Heater Preparation

The test heater is a copper block of 1 cm × 1 cm having 0.3 cm thickness. The copper block has provision to embed the thermocouple, at 0.15 cm from the top surface, to measure the temperature of the copper block. A square resistor of 1 × 1 cm^2 size having 20 Ω resistance is used as a heating element. The resistor is soldered to the bottom of the copper block. The heating element has two leads, which are soldered to copper wires to pass current to the element to provide heating. The copper block is then placed in a polycarbonate substrate and covered by 3M® 1838 Scotch-Weld epoxy on all sides except for the top surface. The epoxy is used to prevent heat loss from sides and bottom of the heater. Epoxy was cured as per the manufacturer's specification. The heater surface temperature is calculated assuming one-dimensional steady-state conduction. To test for the effect of heater size, and orientation, the 1 × 1 × 0.3 cm^3 copper block is replaced with 1.5 × 1.5 × 0.6 cm^3 and 2 cm × 2 cm × 0.8 cm^3 copper blocks. The 1 cm^2, 20 Ω heating element is replaced by a 1.3 cm square, 25 Ω heating element to test for the effect of heater size. All the other steps to prepare the heater remained same. Schematic of the heater assembly used for the pool boiling tests is shown in Figure A.1 (b)

2.2 Experimental Procedures

2.2.1 Nanofluid Preparation Procedures

Previous research by Moreno et al. [11] conducted characterization of nanoparticles using TEM photographing technique and found the average size of nanoparticles to be 27 ± 17 nm. Similar nanoparticles as those used by Moreno et al. [11] were used to prepare nanofluid for all the tests. 0.05 ± 0.004 grams of alumina nanoparticles were weighed using an Acculab VI-1mg balance. All the tests carried out for nanofluid were of 0.025g/L concentration. Base fluid for ethylene glycol and propylene glycol tests were prepared by mixing 400, 600, 800 and 1000 ± 5 ml of ethylene glycol or propylene glycol in water to form two liters of base fluid. Nanoparticles were dispersed in 300 ml of base fluid (water or aqueous solutions of ethylene glycol and propylene glycol of respective concentrations) by mixing the particles in the base fluid and then subjecting the mixture to ultrasonic bath for two hours as mentioned by Moreno et al. [11]. A Cole Palmer Ultrasonic Cleaner Model 08849-00 was used to accomplish this process. After this the 300 ml of nanoparticles + base fluid mixture was added to 1.7 liters of the base fluid to make a total of two liters.

2.2.2 Test Procedures

The test vessel described in section 2.1.1 was thoroughly washed using water before each test. The heater was mounted on the mounting base in the test section and held in place by bolting it to the mounting base. The nanofluid prepared as described in section 2.2.1 was poured into the test vessel described in 2.1.1. The top plate of the test

section was bolted to the body of the vessel using six bolts. Once the vessel was tightly sealed, the two cartridge heaters were turned on and the valve on the top of the vessel was opened to release the dissolved non-condensable gasses from the liquid. Temperature was increased till the liquid reached its saturation temperature and was maintained in the saturated condition for an hour, to avoid presence of any non-condensable gasses in the test liquid. The top valve was then closed and cartridge heaters were turned off. The saturated test liquid was cooled to the required temperature and corresponding saturation pressure using a commercially available fan. Tests were started after allowing the entire mixture to stabilize. An HP6032 power supply was used to supply power to the heater and an HP 3852A data acquisition system was used to record pressure, temperature and power. The power supply and data acquisition system were controlled using a program written in LabView. Tests were conducted till Critical Heat Flux (q''_{CHF}) was reached. The program would check for steady state at each applied heat flux before increasing the heat flux to the next programmed increment. Critical heat flux was determined by the program when the temperature of the heater increases by about 20°C compared to the previous recorded temperature.

2.3 Experimental Uncertainty

Methods described in Kline and McClintock [41] were used to estimate uncertainty. Considering errors due to voltage, surface area of the heater and the current applied, nucleate boiling heat flux uncertainty was estimated to be less than 5%. Temperature measurements were estimated to have less than ± 0.5°C error considering

calibration error. Weight measurements of alumina nanoparticles were estimated to have less than ± 0.004 g error. Uncertainty in liquid volume measurements was estimated be less than ± 5 ml. The net uncertainty in concentration of nanoparticles in base fluid was estimated to be less than ± 0.002g/L.

CHAPTER 3

RESULTS AND DISCUSSIONS

You et al. [8] reported that 0.025g/L concentration of alumina-water nanofluid at T_{sat}= 60°C, yielded an enhancement of about 200% in the critical heat flux. To test the effects of parameters chosen, on the q''_{CHF} of alumina-water nanofluid, this concentration of 0.025g/L was considered.

Since the aim of this research is to study the variations in q''_{CHF}, the experimentally obtained q''_{CHF} is compared with q''_{CHF} calculated using Zuber's correlation [37] for flat plate heater, which is of the form:

$$q''_{CHF} = 0.131 \rho_g^{0.5} h_{fg} [\sigma g (\rho_l - \rho_v)]^{0.25} \qquad \text{eq. (1)}$$

Zuber's correlation is used to predict the q''_{CHF} value for a liquid at saturated conditions, eq (1) yields 561 kW/m^2 as the q''_{CHF} for water at T_{sat}=60° C.

3.1 Effect of Heater Size on q''_{CHF} of Nanofluids

The heater size, pressure, orientation and surface roughness, have shown to effect $q''_{CHF.}$ The following section will discuss the first parameter, followed by the effect of pressure and orientation. However the effect of surface roughness is beyond the scope of this study. Previous research has indicated that an increase in heater size results in a q''_{CHF} decrease for various fluids. To study the effect of heater size on q''_{CHF} of nanofluids, heaters of 1 × 1 cm^2, 1.5 × 1.5 cm^2 and 2 × 2 cm^2 sizes were tested with

water and alumina-water nanofluid of 0.025g/L of alumina nanoparticles concentration at T_{sat}=60°C. The pool boiling curves obtained for the effect of heater size on q''_{CHF} was checked for repeatability with another set of heaters of the same sizes.

Figure A.2 shows boiling curves obtained by testing the three heater sizes. The heater of 1 × 1 cm^2 size showed the maximum q''_{CHF} of the three sizes tested, this was the case not only for pure water but for nanofluids as well. The lowest q''_{CHF} was observed with the 2 × 2 cm^2 size heater. It can be seen from the figure that there is a match between water and nanofluid curves for each size, till the critical heat flux of water, in terms of heat transfer coefficient. In other words addition of nanoparticles does not seem to affect the heat transfer coefficient. From Figure A.2, it can be observed that with increase in heater surface area not only does the q''_{CHF} decrease but the heat transfer coefficient also decreases. In heaters of larger surface area, more number of smaller bubbles collapse into one single bubble before departure. Due to this coalescing of bubbles, the total number of bubbles departing the surface of the heater is reduced. A reduction in the number of bubbles departing the surface means that there is a reduction in the heat transfer from the heater. This coalescing of smaller bubbles into a larger bubble before departure might be the cause for the reduction in the nucleate boiling heat transfer with increase in the size of the heater.

The q''_{CHF} obtained for both water and nanofluid was normalized with respect to Zuber's CHF provided by eq (1) and plotted against L', which is the length of heater surface normalized by the surface tension give by the equation

$$L' = \frac{L}{\sqrt{\sigma / g(\rho_l - \rho_v)}} \qquad \text{eq (2)}$$

Calculation for L' were done by considering the properties of water. Surface tension of alumina-water nanofluid was not measured, and since the amount of nanoparticles added to water is very small, for calculating the L' for nanofluids, the properties of water were used.

Figure A.3 shows the plot of q''_{CHF}/q''_{Zuber} at the L' calculated using eq (2) for the three heater sizes tested. The results show that with increase in L' the q''_{CHF} decreases for both fluids tested (water and nanofluid). In Figure A.3 the data obtained for both the fluids is compared with observations of Saylor et al. [16] and Bar-Cohen and McNeil [17]. It can be observed that the data points obtained with water as the working fluid show a similar trend as observed by other studies. However, the alumina-water nanofluid does not match the correlation due to the fact that there is a drastic reduction in the q''_{CHF} of the 2×2 cm^2 heater unlike water where there is a gradual decrease in the $q''_{CHF.}$ The author speculates that as suggested by Kim et al. [10] there might be an increase in the surface tension due to addition of nanoparticles to water. However, verification for the increase in surface tension cannot be provided as surface tension measurements were not carried out.

Lienhard et al. [14]'s work for the effect of heater size on q''_{CHF} also shows the same trends of decrease in q''_{CHF} with increase in L'. They attribute this reduction in the q''_{CHF} to the number of "vapor jets" present on the surface of the heater. Vapor jets are the columns of vapor formed on the surface of the heater due to the coalescing of

bubbles departing the surface of the heater. Lienhard et al. [14] experimentally proved that the actual number of vapor jets present on the heater can be calculated using

$$\frac{q''_{CHF}}{q''_{CHF\ \text{Zuber}}} = \frac{1.14 N_j}{A_H / \lambda_d^2} \qquad \text{eq (3)}$$

where N_j is the number of jets and λ_d is the wavelength of the vapor jets which can be calculated using

$$\lambda_d = 2\pi \sqrt{\frac{3\sigma}{g(\rho_l - \rho_v)}} \qquad \text{eq (4)}$$

Lienhard et al. [14] suggested the use of eq (3) for calculating effect of heat size on the q''_{CHF} for finite plates. They observed that, for heaters which could only accommodate one vapor jet, eq (3) would hold good, but as the value of L' starts getting larger and larger such that the surface can be considered to be infinitely large the equation proposed by Zuber [37] would hold good. Furthermore, Lienhard et al. [14] suggested that for transition from 1 to 4 jets, 4 to 5 jets and from 5 to 9 jets to take place the area of the heater, A_H, should vary as a function of λ_d. Area of the heater to observe transitions mentioned above can be calculated by the correlations as $A_H = (2\lambda_d)^2$, $A_H = (1+\sqrt{2})^2 \lambda_d^2$ and $A_H = (3\lambda_d)^2$, for transitions from 1 to 4, 4 to 5 and 5 to 9 vapor jets respectively.

Calculations for the number of vapor jets on the surface of the heater were done for the three sizes tested in the present study. Calculations revealed that all the heaters tested have only one vapor jet on the surface. It was estimated that for the transition

from 1 to 4 jets to take place, a heater of 31.36 cm^2 needs to be tested. This particular case of 31.36 cm^2 is beyond the scope of this investigation due to power supply limitations.

Rainey and You [18] tested the effect of increase in heater size with microporous coated heaters and observed the same behavior of decrease in $q"_{CHF}$ with increase in heater size. They attributed this reduction of $q"_{CHF}$ to the fact that with increase in the size of the heater, the fresh liquid that wets the surface of the heater faces a higher thermal resistance from the vapor leaving the surface than in a smaller sized heater. As the heat flux increases the resistance would increase leading to earlier onset of critical heat flux. In heaters of smaller surface area the wetting fluid can reach the center of the heater from sides, whereas in the heater of larger surface area the surface of the heater would have to receive the wetting fluid from the top of the heater due to the fact that the resistance to rewetting flow for a heater is a function of the flow path parallel to the surface of the heater. This being the case the fluid has to cross a higher resistance barrier before making contact with the surface thereby delaying the rewetting time and leading to increase in temperature of the heater giving rise to CHF.

The effect of heater size on $q"_{CHF}$ carried out using three different sizes revealed similar results as observed by other researches for the effect of heater size that: with increase in L' the $q"_{CHF}$ decreases. The author agrees that the reason provided for the decrease in the $q"_{CHF}$ of both water and nanofluids with increase in the size of the heater is due to the reasons provided by Rainey and You [18]. However it can be noticed from the Figure A.2 and Figure A.3 that nanofluids show a higher $q"_{CHF}$ compared to its

counterpart water. Heater of size 1 × 1 cm^2 shows an enhancement of about 190% in the q''_{CHF} over that obtained by Zuber's correlation eq (1), which is close limits of q''_{CHF} enhancement obtained by You et al. [8] and Moreno et al. [11]. Enhancements of ~170% and ~70% were obtained for heaters of 1.5 × 1.5 cm^2 and 2 × 2 cm^2 sizes respectively when compared to q''_{CHF} obtained by eq (1). As mentioned in study by Kim et al. [19] it is still evident that Zuber's correlation to determine critical heat flux, does not predict the critical heat flux of nanofluids correctly.

3.2 Effect of Pressure on q''_{CHF} of Nanofluids

To study the effect of pressure on the q''_{CHF} of nanofluids, tests were conducted at three different saturation pressures, 7.38kPa, 19.94 and 47.39 kPa, on a 1 × 1 cm^2 sized heater. Three different saturation pressures were obtained by varying the cooling time after degassing the test fluid as mentioned in section 2.2.2.

Pool boiling curves obtained for water and alumina-water nanofluid were compared with nucleate boiling curves obtained using Rohsenow's correlation:

$$\frac{C_{pl}[T_{wall} - T_{sat}]}{h_{fg}\,\mathrm{Pr}_l^s} = C_{sf}\left[\frac{q''}{\mu_l h_{fg}}\sqrt{\frac{\sigma}{g(\rho_l - \rho_v)}}\right]^r \qquad \text{eq(5)}$$

where C_{sf} is the combined surface factor, which is different for different liquid-solid interface and for the case of water on emery polished copper is 0.0128; r and s are constants whose values are 0.33 and 1.0 respectively, as suggested by Rohsenow [40].

Results obtained and compared with Rohsenow's correlation are plotted in Figure A.4. From Figure A.4 it can be seen that with increase in pressure both q''_{CHF} and

nucleate boiling heat transfer increase. Similar results of increase in q''_{CHF} and nucleate boiling heat transfer with increase in pressure can be observed in literature. From Figure A.4 it can be seen that nanofluids yield greater q''_{CHF} than water for all the pressures tested. Another interesting observation about the results is the percentage enhancement in q''_{CHF} due to addition of alumina nanoparticles to water to form nanofluid. Maximum enhancement observed was at the lowest pressure (7.38 kPa) tested. Enhancement of about ~230% was observed over q''_{CHF} obtained by Zuber's correlation. Enhancements for higher pressures of 19.94 and 47.39 kPa were about 190% and about 120%, respectively.

Another interesting observation that the author would like to note in Figure A.4 is that, at 7.38 kPa saturation pressure, T_{sat} = 40°C, boiling started at higher heat fluxes compared to the other two pressures tested. The author observed that the bubble departure frequency at 7.38 kPa was lesser compared to departure frequency at 47.39 kPa. Also the shape of bubbles departing the surface at 7.38 kPa was competitively hemispherical compared to the shape of the bubbles at 47.39 kPa. However, these observations cannot be quantified as techniques to measure the bubble departure frequency and bubble size were not employed. The bubble departure takes place from the surface of the heater when the buoyant force of the bubble is capable of exceeding the balanced surface tension around the perimeter of the bubble at the heater surface. The surface tension of water tends to increase with decrease in pressure. The author thinks that this increase in surface tension might be the cause for the bubble to dwell longer on the surface of the heater leading to a decrease in bubble departure frequency

and thereby decreasing the heat transfer rate. Also, the author considers the increase in surface tension and the decrease in bubble departure frequency might be the cause for deviation of the experimentally obtained curve, at 7.38 kPa, from the curve obtained from Rohsenow's correlation in lower heat flux region.

The enhancement in q''_{CHF} due to addition of 0.025g/L of alumina nanoparticles to water, to form nanofluid, can be observed in Figure A.5 where q''_{CHF} obtained experimentally is plotted after normalizing it with q''_{CHF} calculated using Zuber's correlation and plotted for the pressures tested. The author observed that with increase in pressure, the size of bubbles departing the surface of the heater reduced. Moreover, the density of bubbles per unit area increased, which means that there are more nucleation sites per unit area at higher pressure than at lower pressure. This increase in the number of bubbles per unit area and reduction in the size of the bubbles at higher pressure might be the cause for increase in q''_{CHF} and better nucleate boiling heat transfer. However, the above mentioned observations of increase in bubble density, and bubble departure frequency cannot be quantified as techniques to measure the bubble size and bubble departure frequency were not employed. Similar observations of increase in bubble departure frequency and decrease in bubble size were reported by Luke [25] when he tested for the effect of pressure on the q''_{CHF} of propane with copper and steel tubes.

Figure A.6 shows increase in heat transfer coefficient with increase in pressure at various heat flux tested. As mentioned earlier in the discussion, it is evidently seen that with increase in pressure the heat transfer coefficient increases. Similar charts for

increase in heat transfer coefficient with increase in pressure can be seen in study conducted by Nishikawa et al. [23].

The data obtained for the effect of pressure on $q''_{CHF,}$ was used to check for the change in L' due to the fact that L' calculation considers properties such as surface tension, density of the liquid and density of the vapor, which are temperature dependent. Calculations revealed that with change in pressure there is small change in the value of L'. The values obtained for water and nanofluid are plotted in Figure A.7, from the figure it can be seen that there is a change in L' which means that as mentioned by Lienhard et al. [15] eq (2) cannot be used as a "general equation" when attempting to study the combined effect of pressure and heater size on the q''_{CHF}.

3.3 Effect of Orientation on q''_{CHF} of Nanofluids

Earlier work about effect on orientation on q''_{CHF} in saturated nanofluids by Kim et al. [10] was carried out with heater of size 1×1 cm^2. In order to study the effect of orientation on q''_{CHF} with heater of larger size a 2×2 cm^2 heater was used. The heater inclinations were measured with respect to the horizontal. Tests were conducted for water and 0.025g/L concentration alumina-water nanofluid at T_{sat}= 60°C.

As mentioned by Kim et al. [10] the orientation can be divided into three regions; (i) upward facing (0° to 60°) where the bubble departing the surface of the heater departs in a vertical direction into the ambience; (ii) near vertical (60° to 120°) where the bubbles travel a certain distance over the surface before being lodged into the

surrounding and (iii) downwards facing (120° to 180°) where the bubble dwells on the surface for a longer period before departing from the heater surface.

The boiling curves for water at various orientations are shown in Figure A.8. From the figure it can be seen, that as the orientation increases from 0° to 90° the nucleate boiling heat transfer increases and so does q''_{CHF}. A further increase in the orientation from 90° to 135° and 150° shows a reduction in the nucleate boiling heat transfer compared to 90°. Also, the q''_{CHF} is seen to be lower than that for 0°, 45° and 90°. The author observed that with increase in the surface orientation (θ>90°), the size of bubbles increased. However this observation cannot be quantifies as photographic techniques were not applied to measure the size of the bubbles. Similar observations of increase in heat transfer rater with increase in orientation from 0° to 90° were reported by Rainey and You [18]. Rainey and You [18] attributed the increase in heat transfer rate to the fact that with near vertical and vertical heaters, the bubbles formed on the surface of the heater travel a certain distance on the surface of the heater before being discharged into the surrounding. During the travel on the surface, the bubbles tend to drag the entrapped vapor from the surface cavities, thereby causing an increase in the nucleate boiling heat transfer rate. At orientations larger than 90°, the bubble size increase and the bubble departure frequency decreases, this longer dwelling of the bubble and larger size causes higher thermal resistance contributing to lower q''_{CHF}.

Boiling curves obtained at different orientations tested for nanofluids are shown in Figure A.9. A similar trend of variation in the nucleate boiling heat transfer is observed in the lower heat flux region; however after a heat flux of about 600 kW/m^2

the curves seem to collapse. Similar trend of collapsing of the pool boiling curves at different orientations for nano fluid can be seen in earlier work on effect of orientation on q''_{CHF} with nanofluids by Kim et al. [10]; curves obtained by Kim et al. [10] are shown in Figure A.10. Figure A.11 shows the comparison of the obtained data to that of Kim et al. [10]. After normalizing the obtained q''_{CHF} with q''_{CHF} calculated from Zuber's correlation described in eq (1), the enhancement obtained by nanofluids over water is compared. The lower q''_{CHF} of the present study compared to Kim et al. [10] might be due to the increase in heater size. Highest q''_{CHF} was observed at 90° orientation for both water and nanofluid in the current test. However, q''_{CHF} obtained for nanofluid was almost twice of water for the same size heater at 90° orientation. About 80%, 95%, 105% and 120 % enhancement in q''_{CHF} was observed at 0°, 45°, 135°, and 150°, respectively. Maximum enhancement of about 120% in q''_{CHF} over the critical heat flux obtained using Zuber's correlation was observed at an orientation of 150°, similar trends on enhancement was observed in study by Kim et al. [10].

Figure A.12 shows the trend of effect of orientation on enhancements of q''_{CHF} using nanofluid, obtained in earlier work and current study. It is clearly seen that both studies indicate similar trend in enhancement of q''_{CHF} due to addition of alumina nanoparticles to water.

Log scale curves for both water and nanofluid were plotted to understand the behavior at lower heat fluxes. Figure A.13 shows the log scale curves plotted for curves of water and nanofluid obtained at various orientations. From Figure A.13, it can be noticed that, for water case Figure A.13 (a), change in orientation affects the nucleate

boiling heat transfer. Increase in heat transfer coefficient is observed in both upward facing and nearly vertical cases. Similar trends were observed in previous works for the effect of orientation on nucleate boiling heat transfer. However, a slight reduction or no change in heat transfer coefficient is observed in downward facing orientations. Similar results were obtained for nanofluids in Figure A.13 (b). Change in nucleate boiling heat transfer of nanofluids due to orientation is seen only up to a heat flux of ~ 600 kW/m^2. After a heat flux of 600 kW/m^2 all the curves seem to collapse, in other words the orientation seems to have little effect on the nucleate boiling heat transfer. Similar observations for water were obtained by Nishikawa et al. [29], Marcus and Dropkin [28], El-Genk and Guo [39].

3.4 Effect of Anti-Freeze addition on q''_{CHF} of Nanofluids

In many practical applications, the addition of anti-freeze to water is required to prevent freezing. However, addition of anti freeze such as ethylene glycol to water is known to deteriorate the critical heat flux and the nucleate boiling heat transfer [34], [35]. Previous studies on water + ethylene glycol based nanofluids have shown about 130% enhancement in critical heat flux, [11]. This research aims to better understand the behavior of nanofluids with anti-freezes. Two commercially available anti-freezes, ethylene glycol and propylene glycol, are used to study the effect of anti-freeze addition on q''_{CHF} of nanofluids. Tests were conducted on a 1 × 1 cm^2 heater at 60°C. To study the effect of anti-freeze on critical heat flux of nanofluid, 0.025g/L concentration of alumina-water nanofluids was used.

3.4.1 Effect of Addition of Ethylene Glycol

Aqueous solutions of ethylene glycol are used for various heat transfer application, the most common being in automotive radiators as anti-freeze. Moreno et al. [11] investigated the effect of addition of nanoparticles to water and ethylene glycol mixture and observed that with increase in concentration of ethylene glycol up to 30 % by volume the q''_{CHF} reduced. The present investigation broadens the range of the effect of anti-freeze addition on the q''_{CHF} of water + ethylene glycol mixture based nanofluid by testing further concentrations of 40% and 50% by volume concentrations of ethylene glycol compared. Tests were conducted with 1×1 cm^2 size heater at T_{sat}=60°C.

Fig A.14 shows the plot of boiling curves obtained for water + ethylene glycol and water + ethylene glycol based nanofluid of 0.025g/L concentration. It can be clearly noted that as stated by Moreno et al. [11] increase in concentrations of ethylene glycol by volume in water + ethylene glycol mixture does not show significant variations in the $q''_{CHF.}$ The results show behavior similar to that obtained by Van Wijk et al. [36] where negligible or no change was observed with change in the ethylene glycol concentration of the solution. However, deterioration in the nucleate heat transfer rate was clearly seen with increase in concentration of ethylene glycol by volume.

Tests to study the effect of anti-freeze addition on the critical heat flux of water + ethylene glycol based nanofluids have shown enhancements in q''_{CHF} over the estimation provided by Zuber's correlation for water. However, the q''_{CHF} was found to decrease with increase in the concentration of ethylene glycol by volume. About 130% enhancement was observed at 10% by volume concentration of ethylene glycol by

Moreno et al. [11]. The current study saw ~120% and ~80% enhancements in q''_{CHF} at 20% and 30% by volume concentration, respectively. In addition, it can be seen from Figure A.14 that adding nanoparticles to ethylene glycol + water solution did not affect the nucleate boiling heat transfer. However, a reduction in q''_{CHF} was noted with an increase in ethylene glycol concentrations by volume. The enhancement in $q''_{CHF,}$ of the ethylene glycol based nanofluid mixture over aqueous solution of ethylene glycol, observed was about 50% at 40% volume concentration of ethylene glycol. At 50% concentration by volume, enhancement observed was negligible. Figure A.15 shows plot of experimental q''_{CHF} normalized with q''_{CHF} from Zuber's correlation against percentage concentration of ethylene glycol. From Figure A.15 it is clear that an increase in ethylene glycol concentration results in a reduction of q''_{CHF}. During experimentation the author observed that with increase in the concentration of ethylene glycol, precipitation of nanoparticles to the bottom of the test vessel increased.

Such an observation of increase in precipitation with increase in ethylene glycol concentration forced trying of an alternative method to mix the fluids. For the curves shown in Figure A.14, first water + ethylene glycol mixture was prepared. Nanoparticles were dispersed in 300 ml of the water + ethylene glycol mixture. This 300 ml of nanofluid was added to remaining 1700 ml of water + ethylene glycol mixture. The second method of test fluid preparation comprised of first preparing 300 ml of nanofluid by dispersing nanoparticles into 300 ml of pure water and then adding this 300 ml of nanofluid prepared to 700 ml of pure water so as to form one liter of nanofluid. One liter of ethylene glycol was added to one liter of nanofluid and stirred

using a metal stirrer. Only 50% by volume concentration of ethylene glycol was tested. The results obtained by both the methods are plotted in Figure A.16. It can be noted that the second method gave about 30% lower q''_{CHF} than the first method.

3.4.2 Effect of Addition of Propylene Glycol

Figure A.17 shows boiling curves for aqueous solution of propylene glycol based nanofluids at various concentrations. It can be noted that compared to ethylene glycol cases, there is a change in the q''_{CHF} of water + propylene glycol solution with increase in volume concentration of propylene glycol. However, overall trends of change in q''_{CHF} appear to be the same as seen in ethylene glycol tests. Also, there is a clear decrease in the nucleate boiling heat transfer rate with increase in propylene glycol concentration. From the figure it can be seen that water + propylene glycol based nanofluids provide an enhancement in the q''_{CHF} till about 40% by volume concentration. Similar to water + propylene glycol, nucleate boiling heat transfer rate of water + propylene glycol based nanofluids also tends to decrease with increase in propylene glycol concentration. Overall trends observed in water + propylene glycol and water + propylene glycol based nanofluid tests are similar to the trends observed in case of ethylene glycol as the additive. Another interesting fact to be observed is the enhancement in q''_{CHF} due to addition of nanoparticles over that obtained using Zuber's correlation described in eq (1). The maximum enhancement observed was about ~70% at 20% concentration of propylene glycol. Enhancements of about ~ 40% and 25% were observed for 30% and 40% volume concentrations, respectively. Concentration of 50%

by volume showed negligible enhancement in the q''_{CHF}. Irrespective of the concentration, all the mixtures show lower q''_{CHF} values compared to pure water based nanofluid cases, where 190% enhancement over q''_{CHF} obtained from eq (1) was observed on testing alumina- water nanofluid at the same conditions as the other tests. Degradation in the nucleate heat transfer was observed in aqueous solutions of propylene glycol as well as aqueous solution based nanofluid mixture. Clearer understanding of the q''_{CHF} enhancement can be obtained from FigureA.18 where q''_{CHF} obtained is shown after normalizing it with q''_{CHF} from Zuber's correlation eq (1). Figure A.19 has been plotted to compare the trends of both ethylene glycol and propylene glycol.

CHAPTER 4

CONCLUSIONS AND RECOMMENDATIONS

4.1 Conclusions

Pool boiling tests were conducted to study the effect of heater size, pressure, orientation and anti-freeze addition on q''_{CHF} of nanofluids. Nanofluids show higher q''_{CHF} over pure water and q''_{CHF} predicted using Zuber's correlation for water for the parameters tested. As nanofluids show same trends of change in q''_{CHF} and nucleate boiling heat transfer rate as water in most of the cases tested, it is still not clear as to what causes the enhancement of q''_{CHF} due to addition of small quantities of alumina nanoparticles to water and other base fluids tested. The various conclusions that can be drawn from the study conducted are listed below:

(a) When alumina-water nanofluid having 0.025g/L of alumina nanoparticles was tested at T_{sat}= 60°C, the effect of heater size on q''_{CHF} shows a reduction in q''_{CHF} with increase in the size of heater. However, irrespective of the size tested in this study, nanofluids show enhancement. Nanofluids yielded enhancements of ~ 190%, 170% and 70% over q''_{CHF} obtained from Zuber's correlation for water, for heater sizes of 1 × 1, 1.5 × 1.5, 2 × 2 cm^2 respectively.

(b) In the investigation carried out on the effect of pressure on critical heat flux, nanofluids showed behavior similar to the other fluids tested in the past for the effect of pressure on critical heat flux. Critical heat flux (q''_{CHF}) as well as heat transfer

coefficient was found to increase with increase in pressure in the pressure ranges tested. Highest q''_{CHF} obtained was at 47.39 kPa, however, enhancement in q''_{CHF} due to addition of alumina nanoparticles reduced with increase of pressure. Maximum enhancement of ~ 230% was obtained at 7.38 kPa.

(c) The effect of heater surface orientation on q''_{CHF} of nanofluids was tested at five different orientations. It was found that with increase in orientation angle from 0° to 90°, the q''_{CHF} and heat transfer coefficient increase. However, slight changes in both q''_{CHF} and nucleate boiling heat transfer were observed at orientation angles of 135° and 150°. Enhancement due to addition of nanoparticles was found to vary with orientation. Maximum enhancement in q''_{CHF} of ~120% over q''_{CHF} obtained by Zuber's correlation for water was observed at 150° orientation.

(d) Addition of anti-freeze to water has been known to reduce the q''_{CHF} and deteriorate nucleate boiling heat transfer with increase in anti-freeze concentration by volume. Addition of nanoparticles to water + anti-freeze based solution showed an increase in the q''_{CHF} over the q''_{CHF} obtained using Zuber's correlation for water. Enhancements of ~ 120% and 70% were obtained at 20% concentration by volume of ethylene glycol and propylene glycol, respectively.

4.2 Recommendations

This research was conducted to study the parameters affecting the critical heat flux of nanofluids. The parameters tested, heater size, pressure, heater orientation and anti-freeze addition, have shown to affect the critical heat flux in similar ways as they

affect the critical heat flux of water. The author thinks that the following investigations could be carried out to better understand the behavior of nanofluids:

(1) Heater sizes above 32 cm^2 needs to be tested in order to study the transition from one vapor jet to four jets and larger sizes need to be tested to determine the transition length (L'_{trans}).

(2) Temperature limitations of the currently used heating elements did not facilitate testing for q''_{CHF} at higher pressures. Investigations need to be carried out at a pressure of 1 atm and higher to better understand the effect of pressure on nanofluids.

(3) Surface roughness is another key parameter that affects q''_{CHF} and nucleate boiling heat transfer, investigations to study the effect of surface roughness on q''_{CHF} of nanofluids need to be carried out.

(4) This research has tested the effect of only adding anti-freeze, where as investigations to observe the variation in q''_{CHF} due to addition of surfactants could be carried out.

APPENDIX A

ILLUSTRATIONS

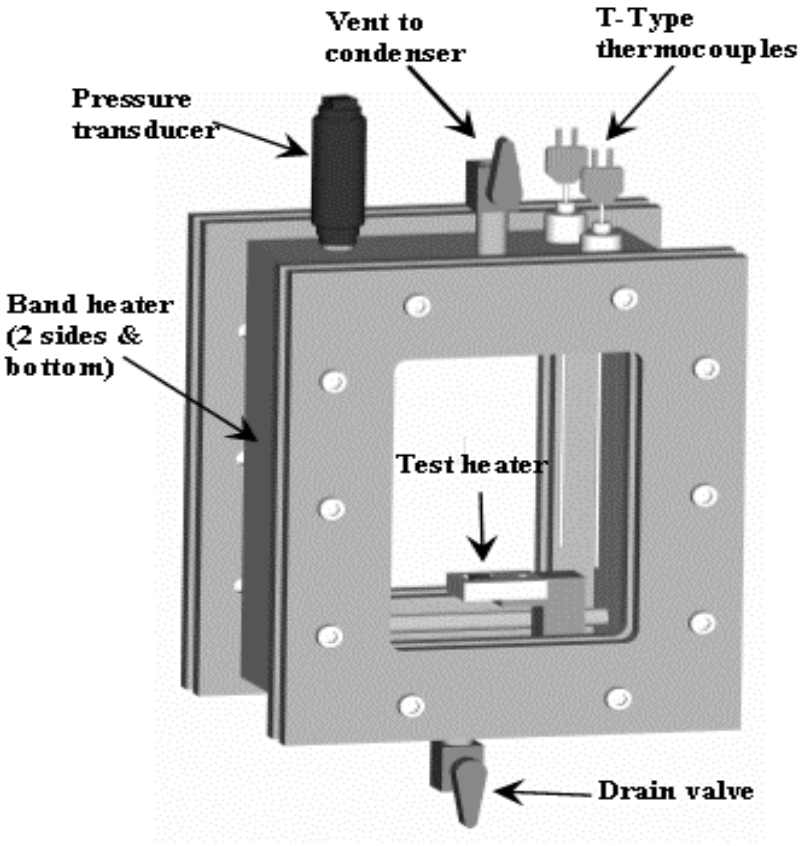

(a)

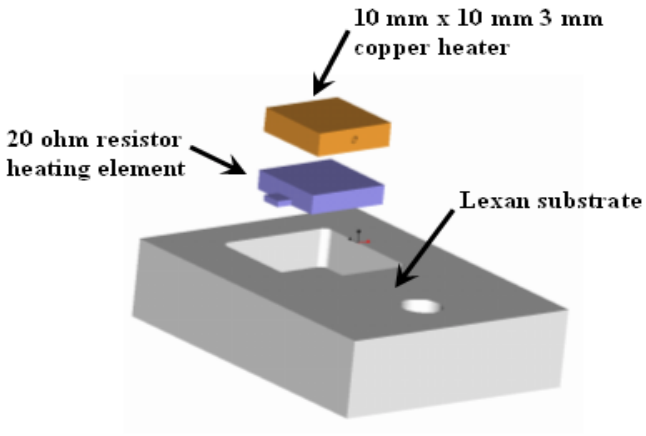

Note: Heaters of size 1.5 × 1.5 cm and 2 × 2 cm had heating element of 25Ω resistor.

(b)

Figure A.1. Schematics of (a) Test Facility (b) General heater

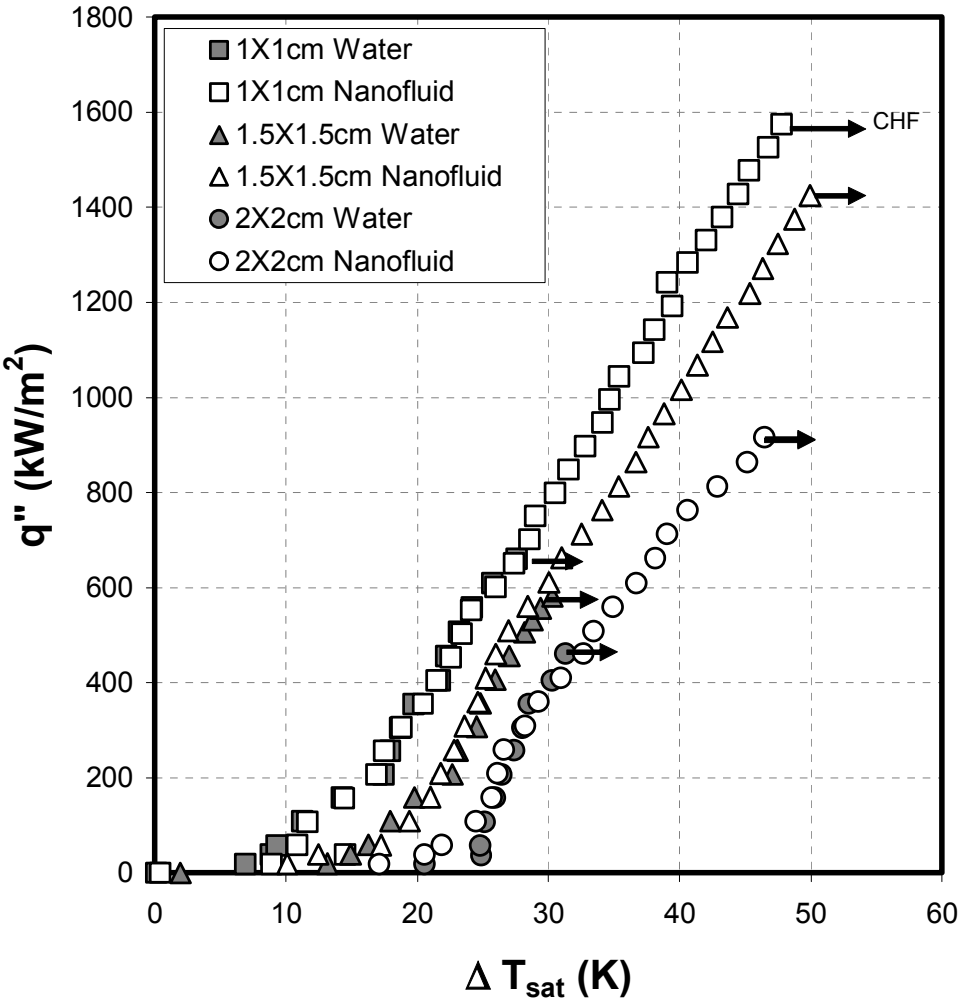

Figure A.2. Pool boiling curves of 1 × 1 cm, 1.5 × 1.5 cm and 2 × 2 cm tested with water and (0.025g/L) alumina-water nanofluid at Tsat=60°C and P=kPa.

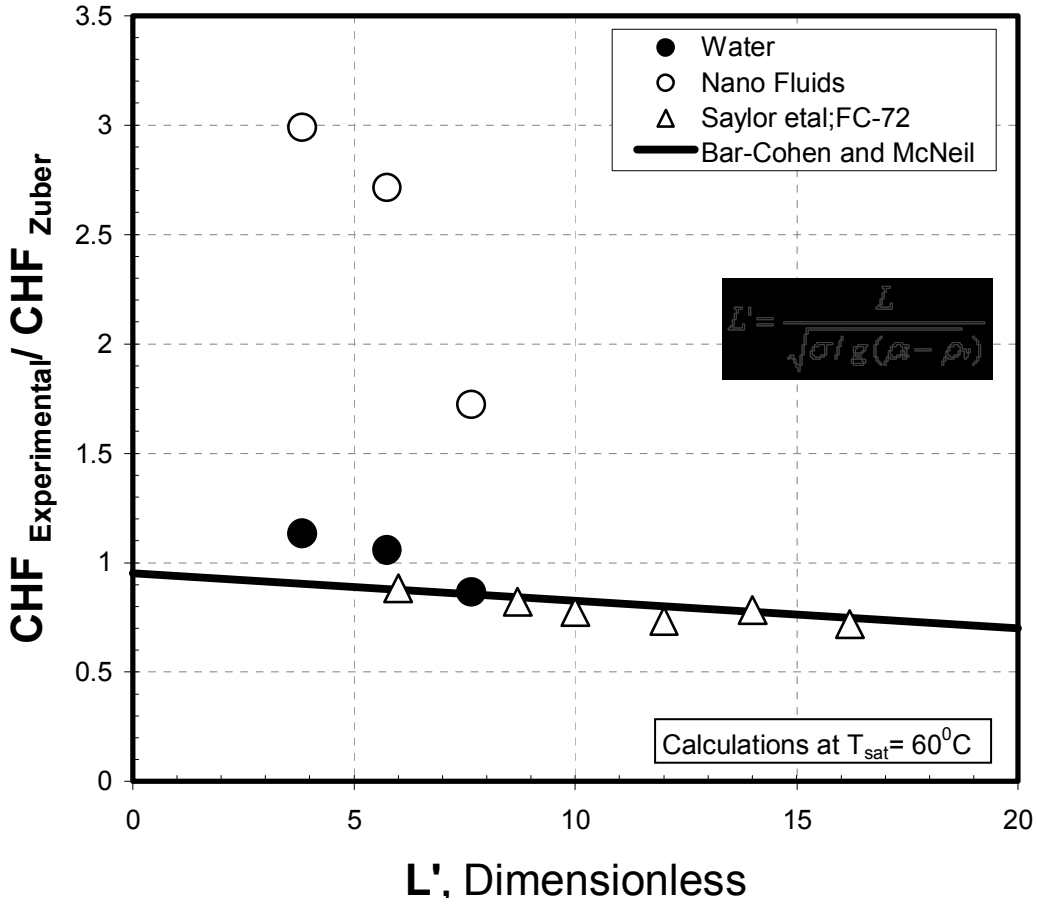

Figure A.3. Critical heat flux ratio of q''_{CHF} obtained with the three sizes to the q''_{CHF} calculated by Zuber's correlation plotted for dimensionless L'.

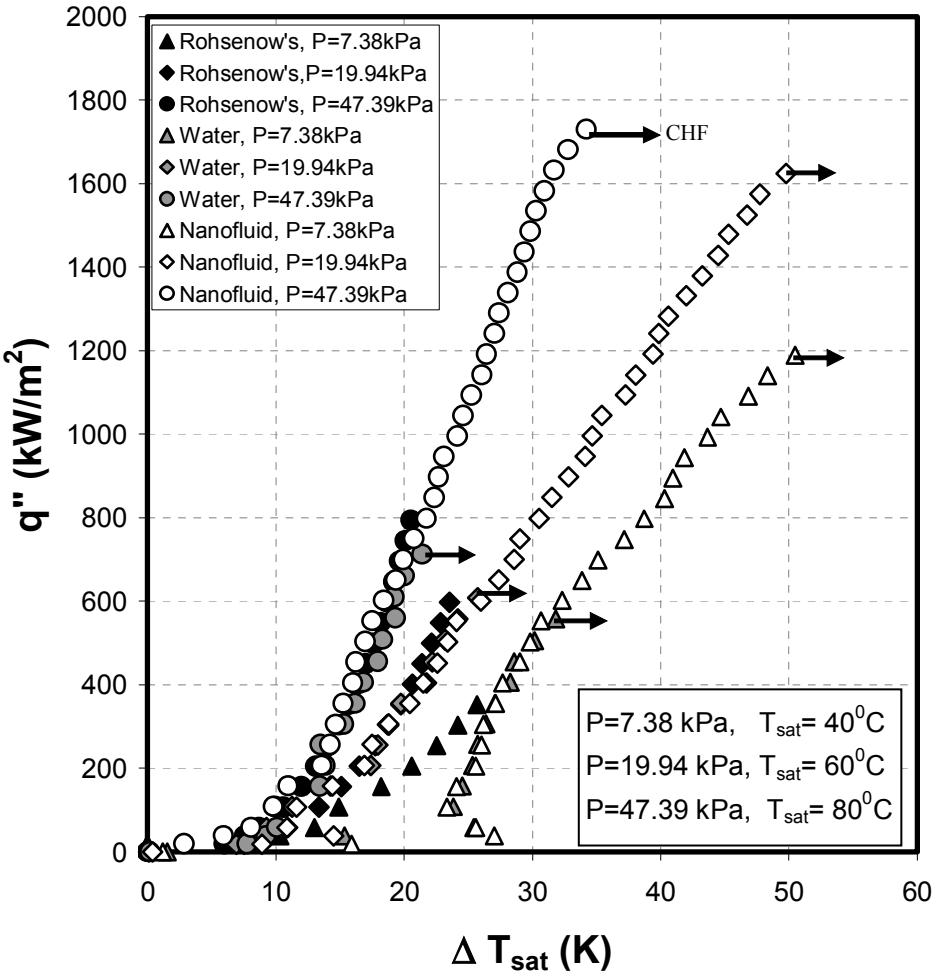

Figure A.4. Boiling curves at 7.38, 19.94 and 47.39 kPa, for water and alumina (0.025g/L)-water nanofluid.

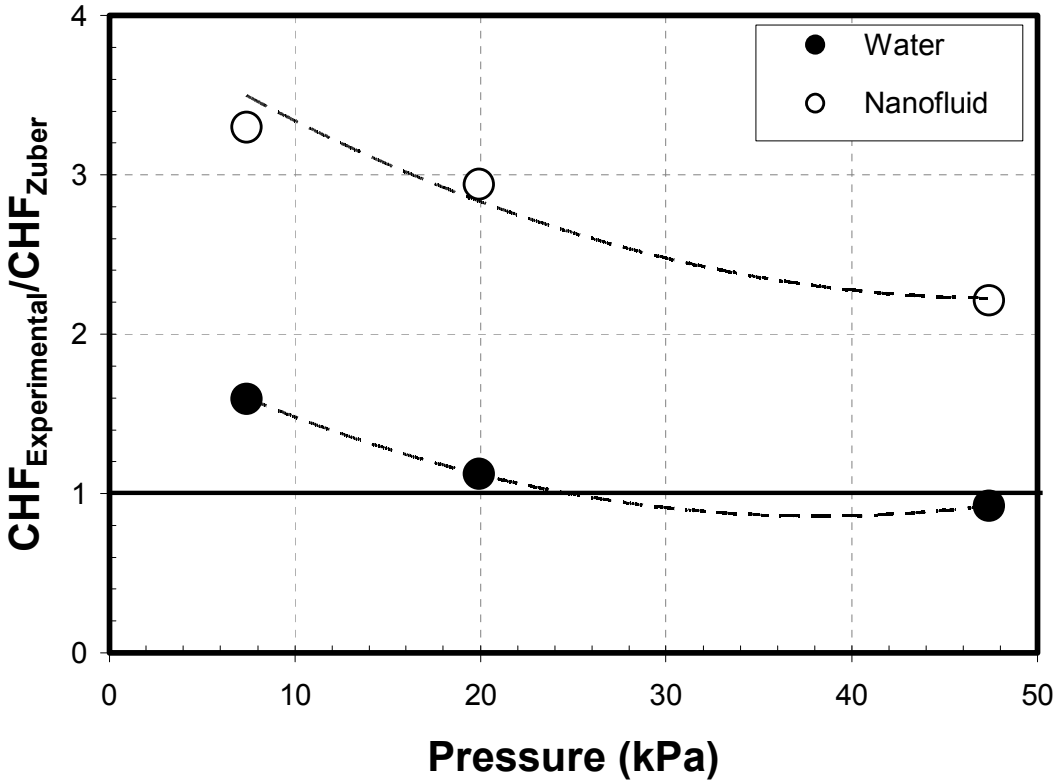

Figure A.5. Normalized q''_{CHF} for tested pressures, showing enhancement of nanofluid over water.

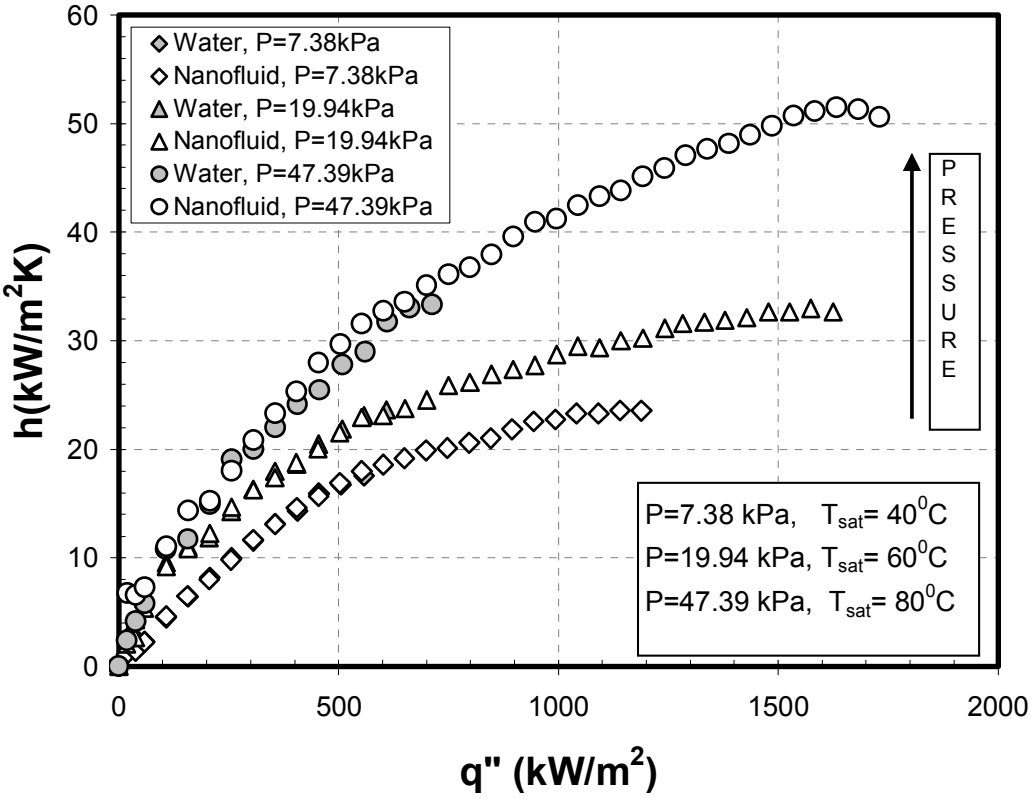

Figure A.6. Increase in heat transfer coefficient 'h' with increase in pressures at various heat fluxes for both fluids (water and nanofluid).

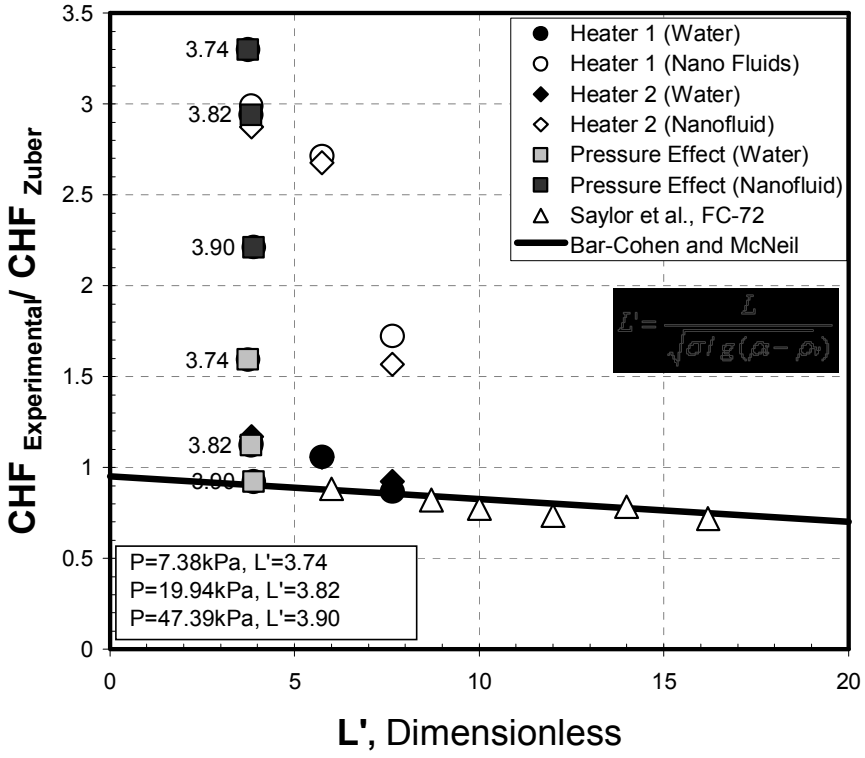

Figure A.7. Plot of q''_{CHF} obtained at various pressures normalized with q''_{CHF} obtained from Zuber's correlation and plotted for dimensionless L'.

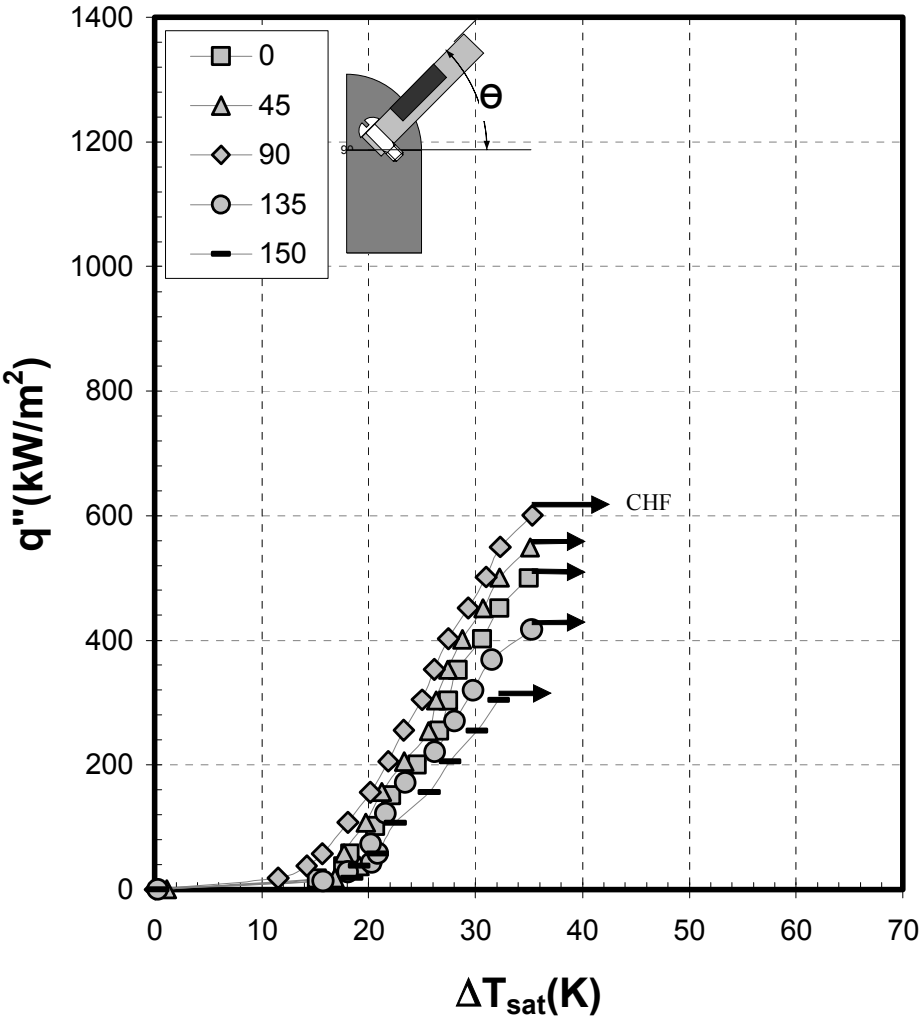

Figure A.8. Boiling curves for water at T_{sat}=60°C, P=19.94kPa, for effect of orientations.

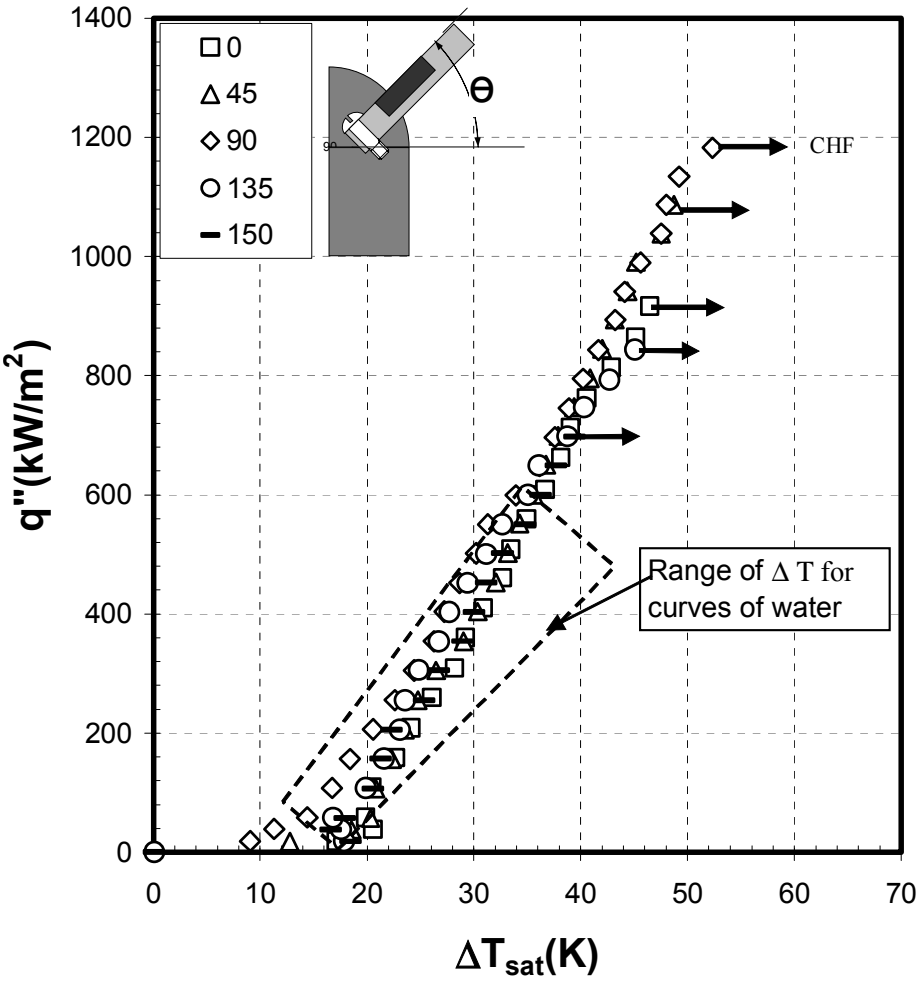

Figure A.9. Pool boiling curves of nanofluids (current study) at various orientations tested at T_{sat}=60°C, P=19.94kPa, with 0.025g/L concentration of alumina nanoparticles.

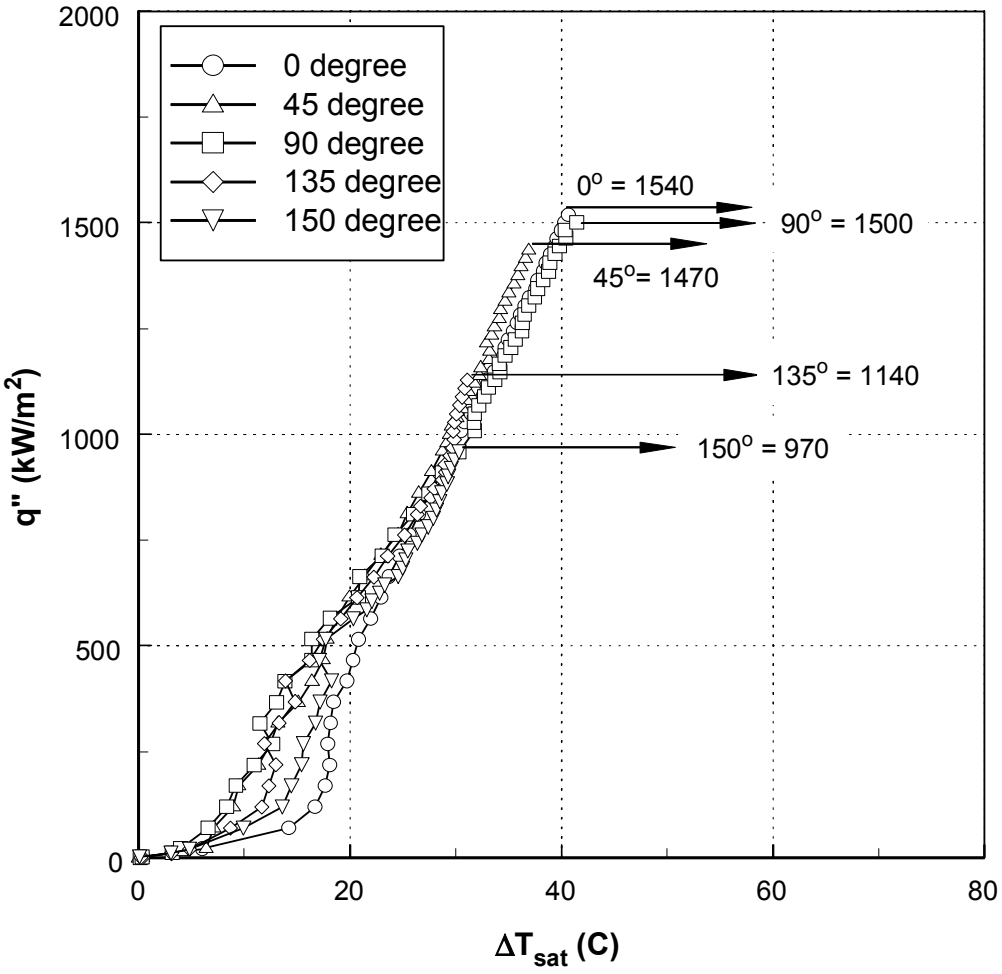

Figure A.10. Pool boiling curves for nanofluids at various orientations obtained by Kim et al. [10]

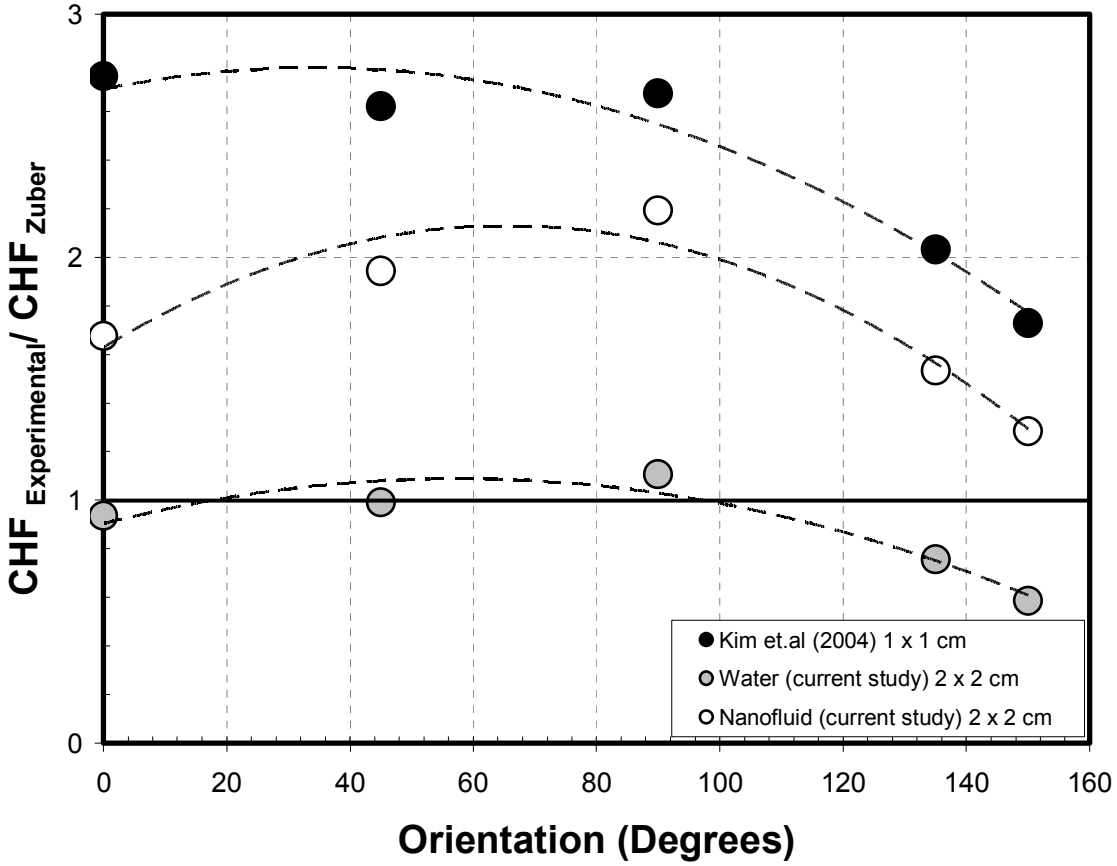

Figure A.11. q''_{CHF} obtained normalized by q''_{CHF} from Zuber's correlation at orientations tested.

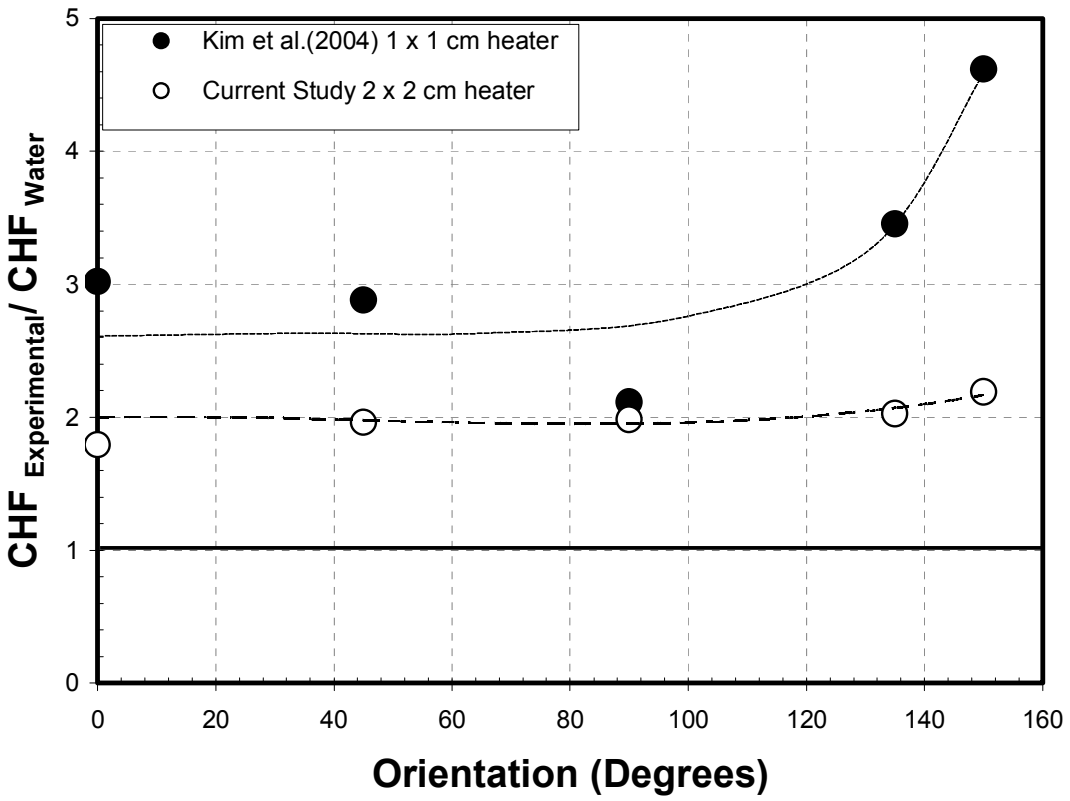

Figure A.12. Comparison of data with Kim et al. [10]

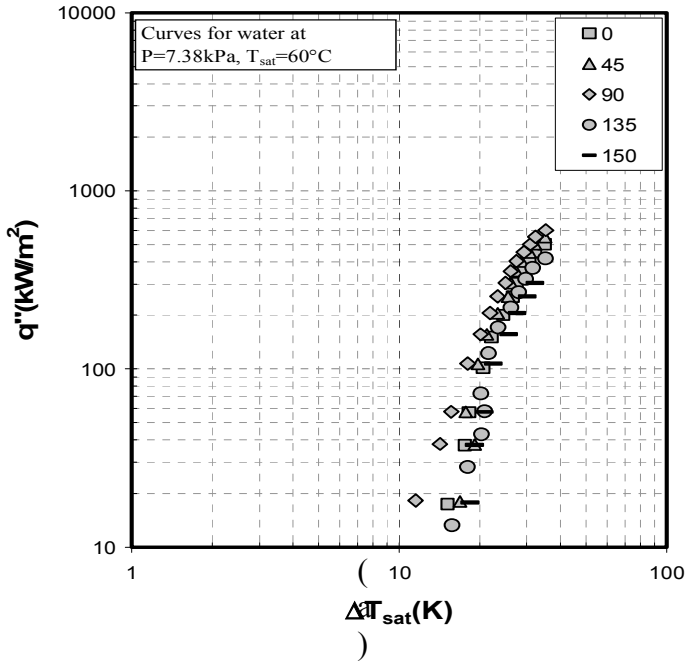

(a)

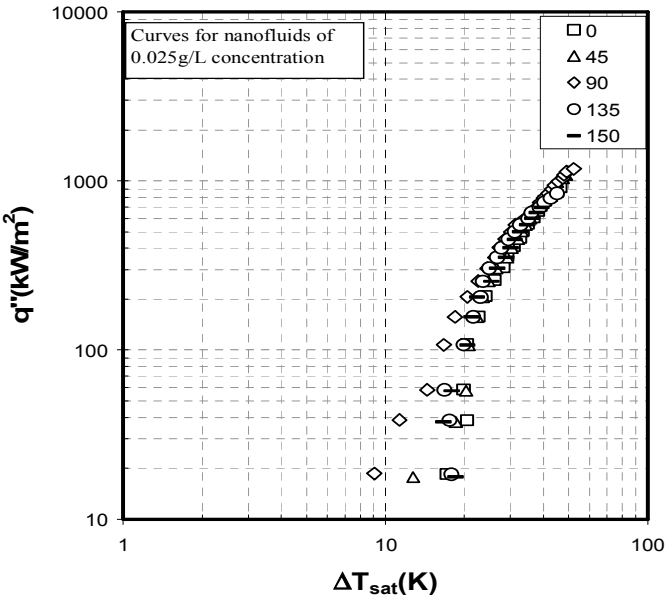

(b)

Figure A.13. Log scale curves for various orientations (a) Water and (b) Nanofluid

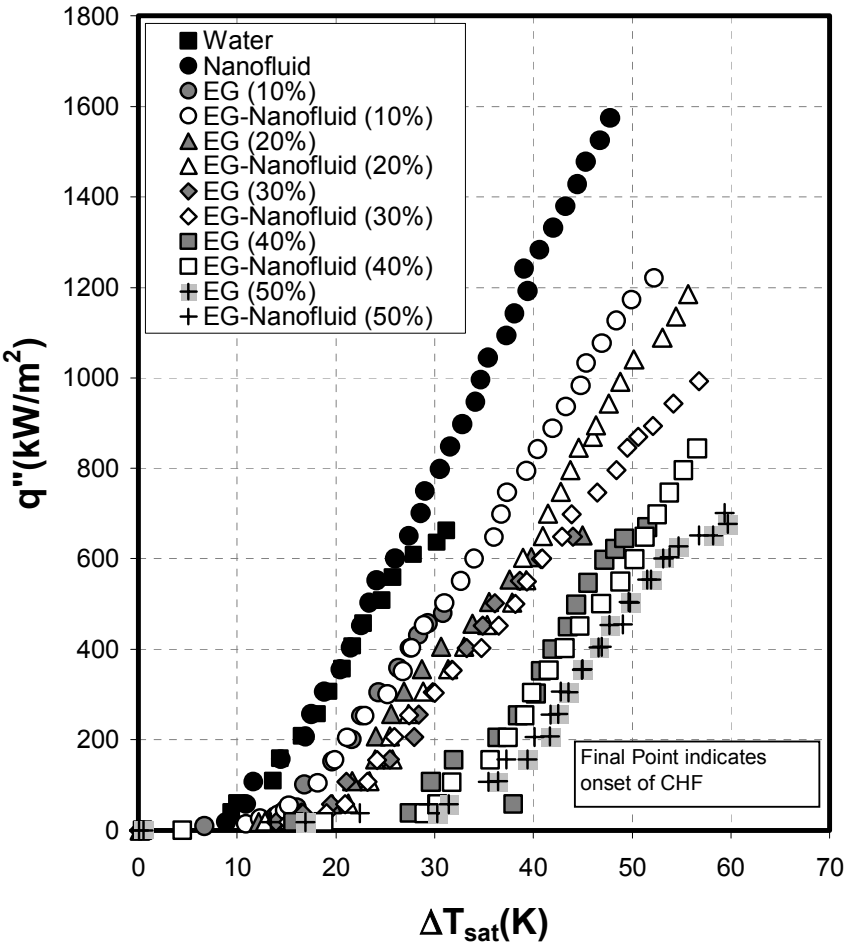

Figure A.14. Boiling curves at various concentrations of aqueous ethylene glycol solution and respective nanofluid.

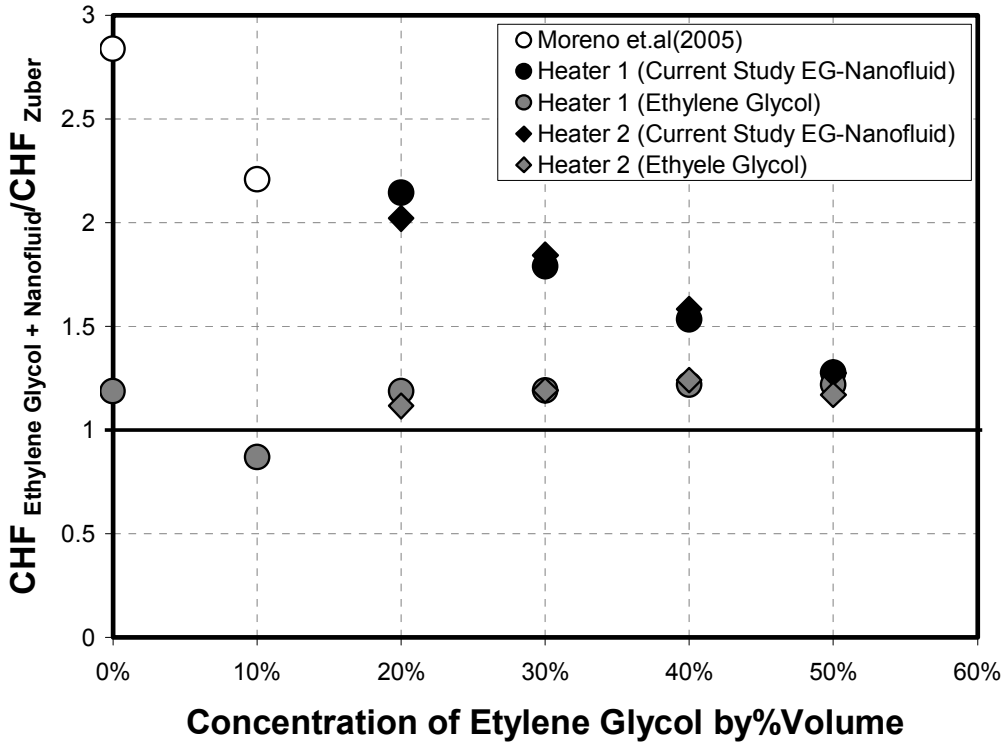

Figure A.15. Normalized q''_{CHF} obtained for both the heaters at various concentrations of ethylene glycol

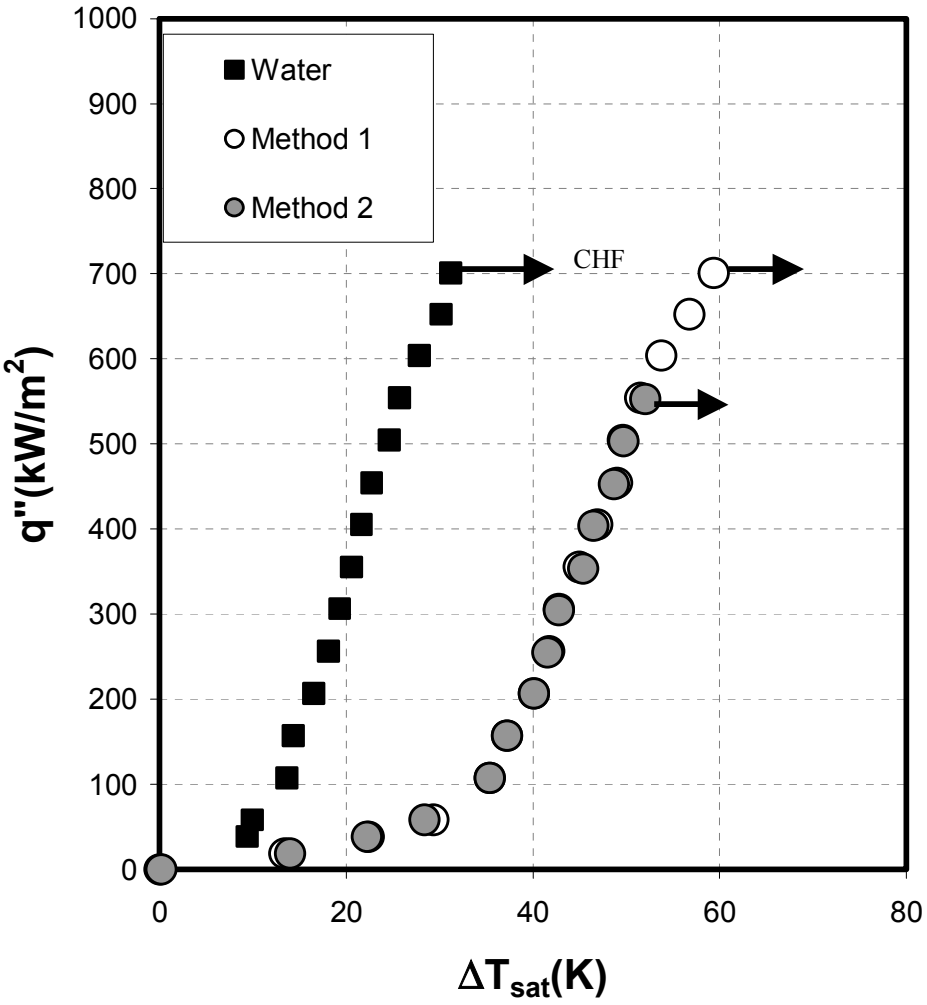

Figure A.16. Boiling curves obtained by different methods of mixing ethylene glycol and nanofluid at T_{sat}=60°C.

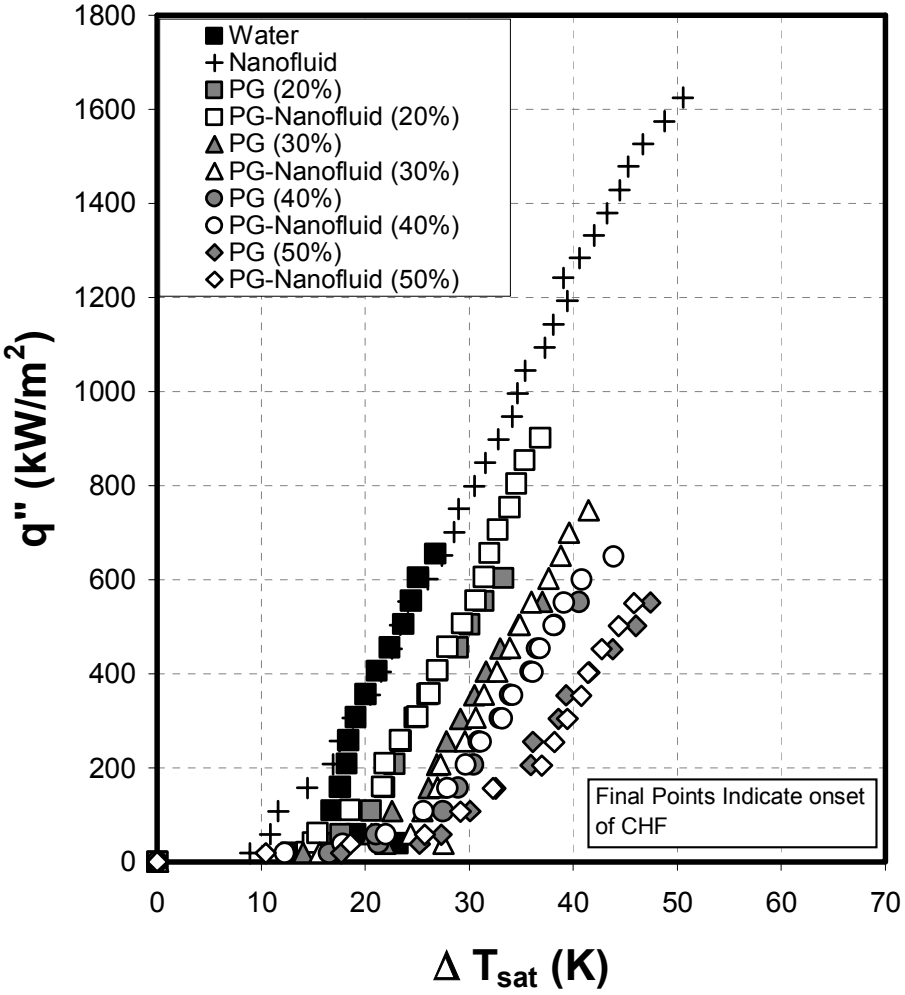

Figure A.17. Boiling curves of aqueous mixtures of propylene glycol and respective nanofluid tested at T_{sat}=60°C.

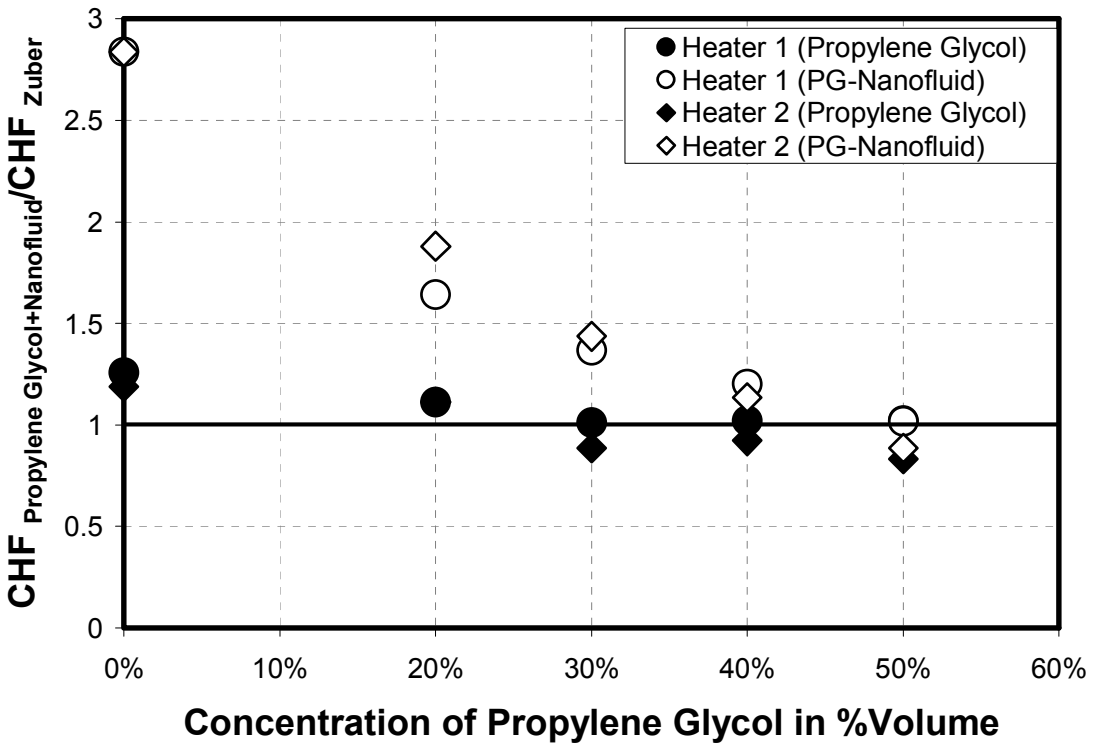

Figure A.18. q''_{CHF} obtained, normalized with q''_{CHF} calculated using Zuber's correlation for water at various concentrations of propylene glycol, for both the heaters tested.

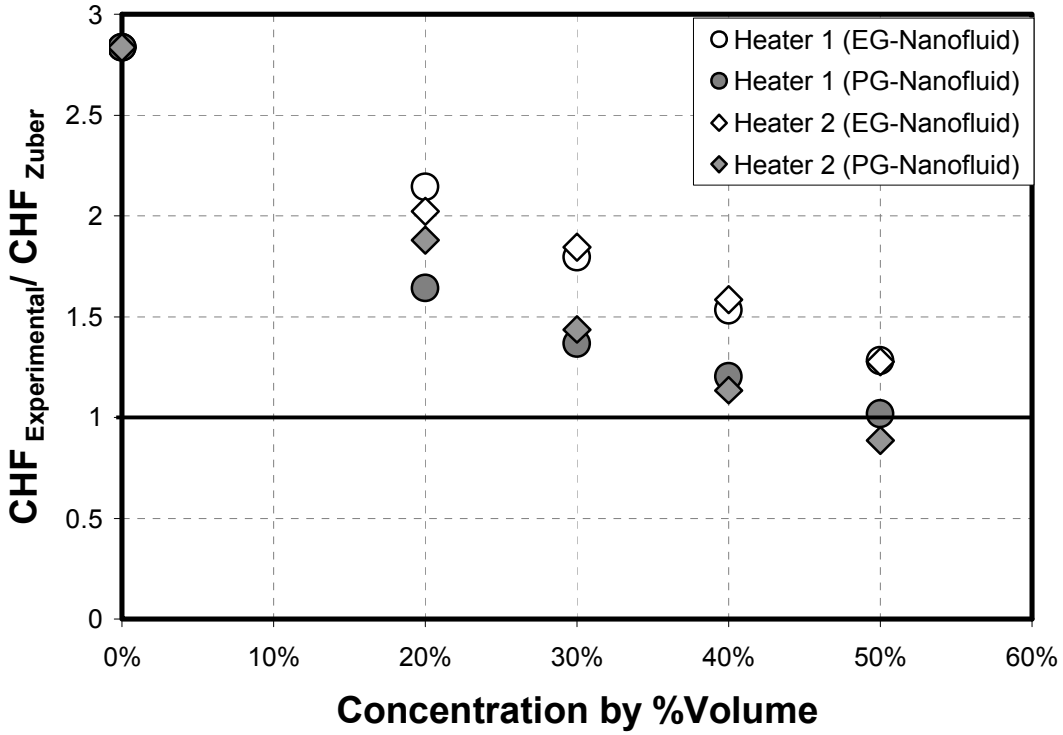

Figure A.19. Comparison of obtained q''_{CHF} of aqueous solutions of ethylene glycol and propylene glycol and their respective nanofluids at concentrations tested.

REFERENCES

[1] Chang, J. Y. and You, S. M. (1997). "Boiling Heat Transfer Phenomena from Micro-Porous and Porous Surfaces in Saturated FC-72," *International Journal of Heat and Mass Transfer*, 40(18), 4437-4447.

[2] Lee, S., Choi, S. U. S., and Li, S. (1999), "Measuring Thermal Conductivity of Fluids Containing Oxide Nanoparticles." *Journal of Heat Transfer*, 121(2), 280-288.

[3] Eastman, J. A., Choi, S. U. S., and Li, S. (2001), "Anomalously Increased Effective Thermal Conductivity of Ethylene Glycol-Based Nanofluid Containing Copper Nanoparticles," *Applied Physics Letters*, 78(6), 718-720.

[4] Choi, S. U. S., Zhang, Z. G., and Yu, W. (2001), "Anomalous Thermal Conductivity Enhancement in Nanotube Suspension," *Applied Physics Letters*, 79(14), 2252-2254.

[5] Liu, M., Lin, M. C. C., and Tsai, C. Y. (2006), "Enhancement of Thermal Conductivity with Cu for Nanofluids using Chemical Reduction Method (Article in Press)," *International Journal of Heat and Mass Transfer*, .

[6] Das, S. K., Putra, N., and Roetzel, W. (2003), "Pool Boiling Characteristics of Nano-Fluids." *International Journal of Heat and Mass Transfer*, 46, 851-862.

[7] Das, S. K., Putra, N., and Roetzel, W. (2003), "Pool Boiling of Nano-Fluids on Horizontal Narrow Tubes," *International Journal of Multiphase Flow*, 29(8), 1237-1247.

[8] You, S. M., Kim, J. H., and Kim, K. H. (2003), "Effect of Nanoparticles on Critical Eat Flux of Water in Pool Boiling Heat Transfer," *Applied Physics Letters*, 83(16), 3374-3376.

[9] Vassallo, P., Kumar, R., and D'Amico, S. (2003), "Pool Boiling Heat Transfer Experiments in Silica-Water Nano-Fluids," *International Journal of Heat and Mass Transfer*, 47, 407-411.

[10] Kim, J. H., You, S. M., and Kim, K. H. (2004), "Pool Boiling Heat Transfer in Saturated Nanofluids," *Proceedings of IMECE Conference,* Anaheim, California.

[11] Moreno, G., Oldenberg, S. J., and You, S. M., Kim, J.H. (2005), "Pool Boiling Heat Transfer of Alumina-Water, Zinc Oxide-Water and Alumina-Water + Ethylene Glycol Nanofluid," *Proceedings of Heat Transfer Conference*, San Francisco

[12] Kutateladze, S. S., and Gogonin, I. I. (1977), "Critical Heat Flux as a Function of Heater Size for Liquid Boiling in Large Enclosure," *Journal of Engineering Physics*, 33, 1286-1289.

[13] Ishigai, S., Inoue, K., and Kiwaki, Z. (1961), "Boiling Heat Transfer from a Flat Surface Facing Downwards," *Proceedings of International Heat Transfer Conference*, 224-229.

[14] Lienhard, J. H., Dhir, V. K., and Riherd, D. M. (1973), "Peak Pool Boiling Heat Flux Measurement on Finite Horizontal Flat Plates," *Journal of Heat Transfer*, 95(4), 477-482.

[15] Lienhard, J.H and Dhir, V.K. (1973), "Hydrodynamic Prediction of Peak Boiling Heat Transfer Fluxes from Finite Bodies," *Journal of Heat Transfer*, 95, 477-482.

[16] Saylor, J. R., Simon, T. W., and Bar-Cohen, A. (1989), "The Effect of a Dimensionless Length Scale on the Critical Heat Flux in Saturated, Pool Boiling." *ASME Publication HTD*-108, 71-80.

[17] Bar-Cohen, A., and McNeil, A. (1992), "Parametric Effects of Pool Boiling Critical Heat Flux in Dielectric Liquids," *ASME Pool and External Flow Boiling*, 171-175.

[18] Rainey, K. N., and You, S. M. (2001), "Effect of Heater Size and Orientation on Pool Boiling Heat Transfer from Microporous Coated Surfaces," *International Journal of Heat and Mass Transfer*, 44, 2589-2599.

[19] Kim, J. H., You, S. M., and Pak, J. Y. (2006), "Effect of Heater Size and Working Fluid on Nucleate Boiling Heat Transfer," *International Journal of Heat and Mass Transfer*, 49, 122-131.

[20] Cichelli, M. T. and Bonilla,C.F (1945), "Heat Transfer to Liquids Boiling Under Pressure," *AIChE*, 755-787.

[21] Lienhard, J. H., and Schrock, V. E. (1963), "The Effect of Pressure, Geometry, and the Equation of State upon The Peak and Minimum Boiling Heat Flux," *Journal of Heat Transfer*, 85(2), 261-272.

[22] Abuaf, N., Balck, S. H., and Staub, F. W. (1985), "Pool Boiling Performance of Finned Surfaces in R-113," *International Journal of Heat and Fluid Flow*, 6(1), 23-30.

[23] Nishikawa, K., Fujita, Y., and Ohta, H. (1982), "Effect of System Pressure and Surface Roughness on Nucleate Boiling Heat Transfer," *Memoirs of the Faculty of Engineering Kyushu University*, 42(2), 95-111.

[24] Mudawar, I., and Anderson, T. M. (1990), "Parametric Investigation into the Effect of Pressure, Subcooling, Surface Augmentation and Choice of Coolant on Pool Boiling in the Design of Cooling Systems for High-Power-Density Electronic Chips." *Journal of Electronic Packaging*, 112, 375-382.

[25] Luke, A. (1997), "Pool Boiling Heat Transfer from Horizontal Tubes with Different Surface Roughness." *International Journal of Refrigeration*, 20(8), 561-574.

[26] Rainey, K. N., You, S. M., and Lee, S. (2003), "Effect of Pressure, Subcooling, and Dissolved Gas on Pool Boiling Heat Transfer from Microporous, Square Pin-Finned Surfaces in FC-72," *International Journal of Heat and Mass Transfer*, 46, 23-35.

[27] Githinji, P. M., and Sabersky, R. H. (1963), "Some Effect of the Orientation of the Heating Surface in Nucleate Boiling," *ASME Journal of Heat Transfer*, 85,(379) .

[28] Marcus, B. D., and Dropkin, D. (1963), "The Effect of Surface Configuration on Nucleate Boiling Heat Transfer," *International Journal of Heat and Mass Transfer*, 6, 863-867.

[29] Nishikawa, K., Fujita, Y., and Uchida, S. (1984), "Effect of Surface Configuration on Nucleate Boiling Heat Transfer," *International Journal of Heat and Mass Transfer*, 27, 1559-1571.

[30] Lienhard, J. H. (1985), "On the Two Regimes of Nucleate Boiling." *ASME Journal of Heat Transfer*, 107, 262-264.

[31] Zuber, N. (1963), "Nucleate Boiling the Region of Isolated Bubbles and Similarity with Natural Convection." *International Journal of Heat and Mass Transfer*, 6, 53-78.

[32] Moissis, R., and Berenson, P. J. (1963), "On Hydrodynamic Transition in Nucleate Boiling," *ASME Journal of Heat Transfer*, 85, 221-229.

[33] Chang, J. Y., and You, S. M. (1996), "Heater Orientation Effect on Pool Boiling of Micro-Porous-Enhanced Surfaces in Saturated FC-72," *ASME Journal of Heat Transfer*, 118, 937-943.

[34] Frea, W. J., Knapp, R., and Taggart, T. D. (1977), "Flow Boiling and Pool Boiling Critical Heat Flux in Water and Ethylene Glycol Mixtures." *Canadian Journal of Chemical Engineering*, 55(1), 37-42.

[35] McGillis, W. R., and Carey, V. P. (1996), "On the Role of Marangoni Effect on the Critical Heat Flux for Pool Boiling of Binary Mixtures," *Journal of Heat Transfer*, 118, 103-109.

[36] Van Wijk, W. R., Vos, A. S., and Van Stralen, S. J. D. (1956), " Heat transfer to boiling binary liquids," Chemical Engineering Science, 66(5) .

[37] Zuber, N. (1959), "Hydrodynamic Aspects of Boiling Heat Transfer," AEC Report No. AECU-4459, Physics and Mathematics.

[38] Carey, V.P.(1992), "Liquid-vapor Phase-Change Phenomena,"

[39] Guo, Z., and El-Genk, M. S., 1992, "An Experimental Study of Saturated Pool Boiling from Downward Facing and Inclined Surfaces," International Journal of Heat and Mass Transfer, 35(9) pp. 2109-2117.

[40] Rohsenow, W.M. (1962), "A method of correlating heat transfer data for surface boiling of liquids," *ASME Journal of Heat Transfer*, 84, 969-975.

[41] Kline, S.J. and McClintock, F.A., 1953 "Describing Uncertainties in Single Sample Experiments," *Mechanical Engineering*, 75(1), pp. 3-8.

BIOGRAPHICAL INFORMATION

Madhav Rao Kashinath obtained his Bachelor of Engineering degree at S.J.C.Institure of Technology, Chickabalapura, affiliated to Visvesvaraya Technological University, Belgaum, Karnataka, India. After graduation he came to United States of America to pursue his Master's in Mechanical Engineering and joined the Microscale Heat Transfer Lab under the supervision of Dr. S.M.You.